



University of Tennessee, Knoxville

TRACE: Tennessee Research and Creative Exchange

Masters Theses

Graduate School

12-1998

Response of a bat to geometrical modifications

Holley Lagay Britton

Follow this and additional works at: https://trace.tennessee.edu/utk_gradthes

Recommended Citation

Britton, Holley Lagay, "Response of a bat to geometrical modifications. " Master's Thesis, University of Tennessee, 1998.
https://trace.tennessee.edu/utk_gradthes/10166

This Thesis is brought to you for free and open access by the Graduate School at TRACE: Tennessee Research and Creative Exchange. It has been accepted for inclusion in Masters Theses by an authorized administrator of TRACE: Tennessee Research and Creative Exchange. For more information, please contact trace@utk.edu.

To the Graduate Council:

I am submitting herewith a thesis written by Holley Lagay Britton entitled "Response of a bat to geometrical modifications." I have examined the final electronic copy of this thesis for form and content and recommend that it be accepted in partial fulfillment of the requirements for the degree of Master of Science, with a major in Mechanical Engineering.

Ahmad Vakili, Major Professor

We have read this thesis and recommend its acceptance:

Ted Paludan, Lou Deken

Accepted for the Council:

Carolyn R. Hodges

Vice Provost and Dean of the Graduate School

(Original signatures are on file with official student records.)

To the Graduate Council:

I am submitting herewith a thesis written by Holley L. Britton entitled "Response of a Bat to Geometrical Modifications." I have examined the final copy of this thesis for form and content and recommend that it be accepted in partial fulfillment of the requirements for the degree of Master of Science in Mechanical Engineering.



Dr. Ahmad Vakili, advisor

We have read this thesis
And recommend its acceptance:

C. J. Paludan

Louis R. Decker

Accepted for the council:



Associate Vice Chancellor and
Dean of The Graduate School

RESPONSE OF A BAT TO GEOMETRICAL MODIFICATIONS

**A Thesis
Presented for the
Master of Science
Degree
The University of Tennessee Space Institute**

**Holley Lagay Britton
November 1998**

DEDICATION

This thesis is dedicated to my parents:

Mr. Charlie M. Britton

and

Mrs. Vera O. Britton

who have given me all the support, love and encouragement

anyone could ever need.

They also gave me invaluable educational opportunities.

ACKNOWLEDGEMENTS

There are many people to whom I am grateful for all their help and guidance over the past two and one half years that I spent at The University of Tennessee Space Institute. I would like to thank my thesis dissertation committee, Dr. Ahmad Vakili, Dr. Ted Paludan, and Dr. Lou Deken. I would particularly like to thank Dr. Vakili for all his help, guidance, suggestions and encouragement. I am deeply grateful.

There are also many of my friends and classmates whose assistance in the preparation of this thesis should be recognized and commended. I would like to especially thank Brett Starr, who taught me how to use COSMOS and who patiently, over the last year, answered all my questions concerning it. I am truly thankful. I would also like to thank Judy Edwards for all her support as a friend and for all her help with computer knowledge and with scanners. Thank you.

I would also like to thank my parents, Charlie and Vera Britton. They were always there for me. Without their constant support, love, and encouragement I would not have achieved all that I have today.

I also owe a great deal to my fiancé, Dennis Bunfield. He was always willing to help no matter what the task. He spent many late nights with me trying to get the plots and pictures in the thesis just right. He never complained. Thank you.

ABSTRACT

An analysis was performed to evaluate the effects of certain geometrical changes to reduce the vibration in the handle of a bat caused by an off node hit. Reducing the vibration is, in a sense, the same as increasing the size of the "sweet spot." A finite element program was used to analyze the bat with and without changes.

Geometrical changes were separately centered in bats at 31.54%, 40.36%, 49.19%, and 58.01% from the barrel end of the bat. A baseline model bat, one with no geometrical change, was also analyzed and used as a basis with which the other bats were compared.

Frequency analyses were performed on all bats. The frequencies for the bat with a geometrical change centered at 31.54% and the bat with a geometrical change centered at 40.36% were lower than the bat with a geometrical change centered at 49.19% and the bat with a geometrical change centered at 58.01%.

A time history analysis was also performed on the baseline bat and the bats with a geometrical change centered at 31.54% and 40.36%. Frequency of the vibration shifted and the amplitude of the oscillations decreased showing that the vibrations were dampened. The bat with a geometrical change centered at 31.54% had the greatest shift in frequency. The damping effect of the vibration changes with the position of the geometrical change. An optimum location for the geometrical change will, therefore, significantly contribute to the dynamics of the bat after the impact with a ball.

A time history analysis was also performed on a bat with a wall thickness of 0.05 inches and a geometrical change centered at 31.54% from the barrel end. These results were compared to the bat with a wall thickness of 0.1 inches and a geometrical change

centered at 31.54% from the barrel end. A displacement versus time curve was used to study the effects of the wall thickness on the frequency and amplitude of vibration. Amplitude of vibration was effected by the decrease in wall thickness. The thinner walled bat had higher amplitude of vibration. Wall thickness does effect the vibration because a thinner walled bat will bend easier and can be displaced more than that of a thicker walled bat.

Measurements were performed with microphones to measure the sound amplitude and frequency of the bat after it had been impacted. A baseline model bat and a bat with a geometrical change centered at 31.54% were measured. Frequency spectrum plots revealed that the baseline model bat had many frequencies. The bat with a geometrical change had a single specific frequency. Therefore, the bat with the geometrical change had less energy lost to vibration.

From analysis performed on the bats, it was apparent that certain geometrical changes are very beneficial to reducing impact vibration. The location of the geometrical change is crucial. With a geometrical change centered at an optimum location in a bat, the vibration in a bat would be reduced. With the addition and optimum location of the geometrical change in a bat, the frequency of vibration in a bat begins to shift and the amplitude of the oscillations begin gradually reducing quicker. If a geometrical change is centered in a bat at an optimum location, vibration will be reduced as if the "sweet spot" had been increased.

TABLE OF CONTENTS

CHAPTER		PAGE
1.	INTRODUCTION	1
2.	BACKGROUND	3
	2.1 Introduction.....	3
	2.2 Wood versus Aluminum	4
	2.3 Sweet Spot	6
	2.4 Center of Percussion	7
	2.5 Vibration	7
	2.6 Clamped Versus Unclamped.....	26
	2.7 Impact Energy Test	31
	2.8 Summary of Reviews.....	38
3.	COSMOS	39
	2.1 Introduction.....	39
	2.2 GEOSTAR	39
	3.3 STAR	40
	3.4 DSTAR	42
	3.5 ASTAR	45
4.	PROCEDURE.....	48
	4.1 Introduction.....	48
	4.2 Drawing.....	48
	4.3 Meshing.....	49
	4.4 Material Properties.....	52
	4.5 End Caps	52
	4.6 Displacements	55
	4.7 Loads.....	56
	4.8 Geometrical Changes	56
	4.9 Analysis.....	58
5.	RESULTS	61
	5.1 Linear Static Analysis	61
	5.2 Frequency Analysis.....	63
	5.3 Post Dynamic Analysis	76
	5.4 Experiment.....	94
6.	CONCLUSION.....	100
	BIBLIOGRAPHY.....	103

VITA.....	106
-----------	-----

LIST OF TABLES

TABLE	PAGE
1. Bat Displacements	61
2. Natural frequencies for baseline model bat and for bats with a geometrical change centered at 31.54%, 40.36%, 49.19%, and 58.01% from the barrel end	64
3. Aluminum geometrical change frequency versus acrylic geometrical change frequency	72
3. Percentage variations in frequency from baseline model bat for bats with different wall thickness	73
5. Percentage variations in frequency from baseline model bat for bat with a geometrical change centered at 31.54% from the barrel end of the bat	75

LIST OF FIGURES

FIGURE	PAGE
1. Response of Rigid and Wooden Bat	5
2. Frequency Plot	15
3. First two modes for a free-free beam	16
4. First two modes for a cantilever beam with one end clamped and one end free	17
5. First two modes for a fixed-fixed beam with both ends clamped.....	18
6. Effect of span length on mode of vibration.	19
7. Antinodes and Nodes	20
8. Pain Ratings Caused from the Sting of the Bat.....	22
9. Cross-Section of Ball as it Impacts Bat at Different Velocities.....	24
10. Trampoline Effect Occurring when Ball Impacts a Bat.....	25
11. Bat's Lowest Modes of Oscillation.....	27
12. Oscilloscope Traces Showing Vibration of a Bat with its Handle Clamped in a Vise (Upper Trace) and a Bat that is Hand Held (Lower Trace).....	28
13. Oscilloscope Traces Showing the Vibration of a Bat with its Handle Clamped in a Vise.....	29
14. Load and Energy Curves with Respect to Time for a Bat Impacted 2 Inches from the Barrel End	32

15.	Load and Energy Curves with Respect to Time for a Bat Impacted	
	3 Inches from the Barrel End	33
16.	Load and Energy Curves with Respect to Time for a Bat Impacted	
	4 Inches from the Barrel End	34
17.	Load and Energy Curves with Respect to Time for a Bat Impacted	
	5 Inches from the Barrel End	35
18.	Load and Energy Curves with Respect to Time for a Bat Impacted	
	6 Inches from the Barrel End	36
19.	Load and Energy Curves with Respect to Time for a Bat Impacted	
	7 Inches from the Barrel End	37
20.	Model Drawing of the Bat used in the COSMOS Analysis.....	55
21.	The Locations of the Referenced Nodes on the Bat	63
22.	Mode 1 deformed shape for the baseline model bat	65
23.	Mode 2 deformed shape for the baseline model bat	66
24.	Mode 3 deformed shape for the baseline model bat	67
25.	Mode 1 deformed shape for the bat with a Geometrical	
	Change Centered at 31.54%.....	68
26.	Mode 2 deformed shape 2 for the Bat with a Geometrical	
	Change Centered at 31.54%.....	69
27.	Mode 3 deformed shape for the Bat with a Geometrical	
	Change Centered at 31.54%.....	70
28.	Bat with the new mesh.....	74

29. Vibrational Amplitude Versus Time for a Bat struck in the Barrel	
Region.....	77
30. Displacement Versus Time Curves for the Baseline Model Bat	79
31. Displacement Versus Time Curves for the Bat with a Geometrical	
Change Centered at 31.54% from the Barrel End of the Bat.....	81
32. Displacement Versus Time Curves for the Bat with a Geometrical	
Change Centered at 40.36% from the Barrel End of the Bat.....	83
33. Combined Displacement Versus Time Curves. for the Baseline.....	86
34. Displacement Versus Time Curves for the Bat with a Wall	
Thickness of 0.05 Inches and Containing a Geometrical	
Change Centered at 31.54% from the Barrel End of the Bat.....	89
35. Displacement Versus Time Curves for the Bat with a Wall	
Thickness of 0.05 Inches and for the Bat with a Wall	
Thickness of 0.1 Inches.....	92
36. Experiment Setup for Measuring the Sound Amplitude of a Bat	
After Impact.....	94
37. Fourier Transform of the Sound Amplitude for the Baseline Model	
Bat.....	96
38. Fourier Transform of the Sound Amplitude for the Bat With a	
Geometrical Change Centered at 31.54% from the Barrel	
End of the Bat	98

1. INTRODUCTION

Anyone who has ever picked up a baseball or softball bat and hit a ball has felt the sting of the bat. When a ball hits a bat it causes a vibration in the bat. This vibration is felt in the handle and consequently in the hitter's hands. This vibration can be greatly reduced if the ball strikes the bat at one of the bat's sweet spots, a point on the bat where maximum energy is transferred from the bat back into the ball after impact.

For years, the manufacturers of bats have been improving and optimizing their product. One very important optimization in the design of a bat would be a design that reduced the handle vibration. The handle vibrates less when the bat is impacted at a sweet spot. Increasing the size of this sweet spot would be a great advancement in the technology of bats.

Adding geometrical changes to the hollow inside the bat is one method for trying to increase the size of the sweet spot. This method increases the size of the sweet spot without changing the outer design or dimensions of the bat. The geometrical change results in a change the inner circumference of the bat. The geometrical change acts as a damper and a tuner. It absorbs some of the vibration when the ball does not impact the bat at the sweet spot; and it focuses the energy to select frequencies.

The problem arises in finding the optimum size and location for the geometrical change. In order to find the optimum location, a trial and error method can be used. Geometrical changes of different sizes are centered at varying locations in the bat. Analysis must then be performed on the bat for each location of the geometrical change.

Once the optimal location for the geometrical change is found, the result is reduced vibration in the handle and less sting felt in the batter's hands. Therefore, the addition of this optimally placed geometrical change has, in a sense, increased the size of the sweet spot.

2. BACKGROUND

2.1 INTRODUCTION

Baseball and softball bats have been around for as long as little boys and little girls have been hitting rocks and balls over fences. They have come a long way since the first sticks and rake handles that were once used for sending a ball into the outfield. For as long as bats have been in existence, people have been trying to improve their design and performance. Today, bats are made of various materials such as aluminum and wood. They are also much lighter and more flexible than the bats of yesteryear. Even though bats have made a lot of progress, there is still plenty of room for improvement.

Many methods have been used to optimize the design and performance of a bat. Perhaps one of the greatest improvements that could be made is increasing the bat's sweet spot. When designing a bat, it is very important to locate the sweet spot so that the performance of the bat is optimal. The sweet spot will be explained later in this chapter. The sweet spot is directly related to the vibration felt in a bat's handle when the ball is struck. Thus, reducing this handle vibration is another crucial aspect to improving the bat. A higher performance bat is one that has a bigger sweet spot and one that transports more energy into the ball rather than into the batter's hands when the sweet spot rebounds (Tognarelli and Dunbar, 1994).

The study of the handle vibration in the bat is important when determining the location and importance of the sweet spot. In order to study the vibration, a model of the bat is constructed. When modeling a bat for analysis, it must first be determined whether

the bat handle is clamped or unclamped. An impact energy test has been used in the past to study the correlation between hitting the sweet spot and the handle vibration (Dunbar and Tognarelli, 1994).

2.2 WOOD VERSUS ALUMINUM

The first bats were made from hickory. In 1890, however, northern white ash became the leading wood in bat production. This type of wood is used because it is a lightweight, hard, tough wood that has more whip action. This whip action causes the ash bats to crack easier (Schuessler, 1994).

Aluminum is often used today in nonprofessional games because it is more durable and generates more power than a wooden bat. For example, a swing that produces a 380-foot home run with a wooden bat will produce a 415-foot home run with an aluminum bat (Adair, 1990). They do not break like a wooden bat; instead, they “crack, dent, and lose their pop as they fatigue during hitting” (Ashley, 1995).

The hollow aluminum bat is also more rigid than the solid wooden bat. Usually, “the aluminum bat is twice as stiff as the wooden bat; twice as much force is required to bend it to a given amount” (Adair, 1990). Since the aluminum bat is stiffer than the wood bat, there will be less longitudinal vibration in the aluminum bat than in the wooden bat when it is struck near a sweet spot. In other words, the aluminum bat will sting the batter’s hands less than a wooden bat when there is an off node hit (Adair, 1990).

An aluminum bat also has a higher vibrational frequency than a wooden bat. This results in more energy being transferred to the ball from the bat. This is why a ball can be hit farther with an aluminum bat than with a wooden one by the same person. “The response of the aluminum bat to a ball hit away from the vibrational node (or sweet spot) is close” to the response of a perfectly rigid bat (Adair, 1990). This response can be seen in Figure 1 (Adair, 1990).

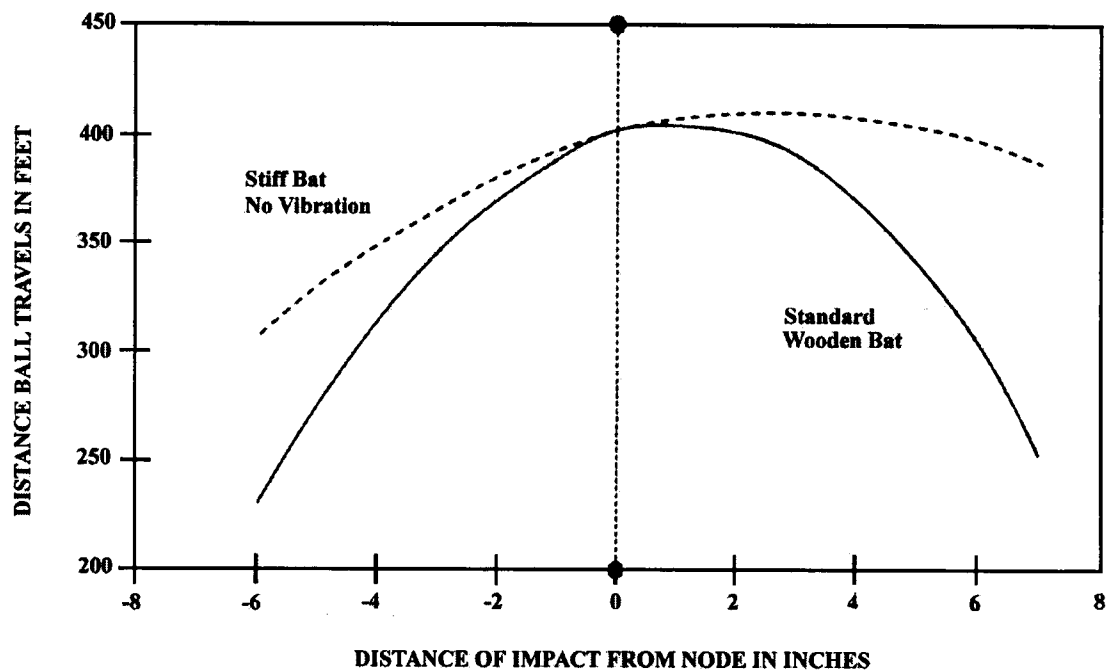


Figure 1: Response of rigid and wooden bat (Adair, 1990).

David C. Cook has designed a three-piece wooden bat that was as durable as an aluminum bat and had the performance of a wooden bat. Cook called his bat the Dream. It consisted of a 23-inch white ash handle, 7-inch hickory barrel, and a 3-4 inch maple end. “Glued serrated finger joints” hold the bat together. The sweet spot on the Dream is

larger than a sweet spot on other wooden bats because the three different woods with their different densities optimally balance the bat. The Dream bat is much more durable than other wooden bats. It also has less vibration than ordinary wooden bats. The ash handle and the finger joints absorb part of the vibration when a ball hits the bat (Ashley, 1995).

Today's bats are also a lot lighter and smaller overall than the bats used in Babe Ruth's day. For example, the bat Babe used, early in his career, weighed 52 ounces; and, at the time of his retirement, he was using a much smaller bat weighing 38 ounces. The aluminum bats of today weigh as little as 26 ounces (Schuessler, 1994).

2.3 SWEET SPOT

The sweet spot on a bat is the point that "provides the most energy reflectivity with minimal absorption" (Dunbar and Tognarelli 1994). When the ball strikes a sweet spot on the bat it will travel farther and have less handle vibration (Dunbar and Tognarelli 1994). Hitting a sweet spot on a bat will "result in maximum transfer of energy from the bat to the ball, maximizing the post impact velocity for a given collision" (Noble, 1983). A bat has two sweet spots, the center of percussion and the node of the first harmonic (Brody, 1985).

The vibration in the handle occurs when the higher harmonic of the bat's natural oscillation has been excited. The higher harmonic is not excited when the ball strikes the bat at the sweet spot. This sweet spot is at the node of the first harmonic. It can be found by holding the bat on both ends and thumping it. A resonance will sound unless the bat is thumped at this node (Brody 1985).

2.4 CENTER OF PERCUSSION

The center of percussion on a bat is the point where when struck there is “no reaction force at the axis” (Noble 1983). In other words, no momentum is transferred to the bat’s handle (Adair, 1990). The axis is the point around which the bat is free to pivot during an impact of a bat and a ball. The reaction force axis is independent of the bat’s rotational axis during the swing of the bat. In order to find the center of percussion, the reaction force axis must be found. This axis is located on a bat’s handle touching the hitter’s hands. The center of percussion is determined by

$$q = \frac{k^2}{r} = \frac{I}{mr}$$

where q is distance from axis to center of percussion, k is the radius of gyration, I is the moment of inertia, m is the mass, and r is the distance from axis to center of mass. The center of percussion is a sweet spot on a softball or baseball bat (Noble, 1983).

2.5 VIBRATION

When any object strikes another object, there is a transfer of momentum. The game of pool is a good example of this concept. When the cue ball strikes the stationary eight ball, the momentum from the cue ball is transferred into the eight ball. The eight ball propelled by the transferred momentum from the cue ball then begins to roll in the initial direction of the cue ball. If there is a complete transfer of momentum upon contact, the cue ball stops. If there is not a complete transfer of momentum, the cue ball will also continue to roll. The equation for linear momentum is

$$L_i + \int_{t_i}^{t_f} R dt = L_f$$

where L_i represents the initial linear momentum, $\int_{t_i}^{t_f} R dt$ represents the resultant of all linear impulses that are applied to the object, and L_f represents the final linear momentum (Riley and Sturges, 1993). If the sum of the linear impulses are zero, then linear momentum equation is written as

$$L_i = L_f$$

where L_i represents the initial linear momentum and L_f represents the final linear momentum (Riley and Sturges, 1993). This is the principle of conservation of linear momentum equation. Linear momentum is conserved in one direction. Therefore, when a cue ball strikes the eight ball and then continues in the same direction, linear momentum is conserved. However, when a ball strikes a bat it is sent flying back in the opposite direction. The velocity after impact is opposite to the velocity before impact. The final momentum is negative with respect to the initial momentum.

There is also a transfer of energy when two objects come in contact with each other. When a ball impacts a bat, energy is transferred. The conservation of energy equation is stated as

$$T_1 + V_1 = T_2 + V_2$$

where T_1 and T_2 represent the initial and final kinetic energy and the initial and final potential energies are represented by V_1 and V_2 . The sum of T and V is called the total mechanical energy (Riley and Sturges 1993). The conservation of energy is a special

case; usually some of the energy is not transferred when two bodies collide. If all of the energy is not transferred into the contacting body, some of the energy will be lost or left in the initial body. When a ball impacts a bat, the energy that is not transferred into the ball after the impact is left in the bat. This energy causes the bat to vibrate.

What is vibration? When an object has any form of repeated oscillations about an equilibrium point, it is vibrating, and this is a mechanical vibration. Mechanical vibrations are often caused by outside forces coming in contact with an object in equilibrium. A diving board is a good example. When a person dives off the board, a force is applied to the board by the jumping motion of the diver. The board is forced down past the equilibrium position. Once the diver has left the board, the board then springs back to the equilibrium position. However, the board has velocity and it passes through the equilibrium position. As long as there is velocity in the board, this process will repeat. The forces in the board try to restore the board to its equilibrium position. When a ball impacts a bat, the diving board example can be used to describe the impact. The ball represents the diver and the bat represents the diving board. The ball is the force that causes the bat to pass through its equilibrium position. The bat trying to return to its initial equilibrium position is felt in the form of vibration in the handle. The vibration in the handle is a direct result of the energy that was lost in the impact.

2.5.2 Forced and Free Vibrations

There are two different types of vibration: forced and free. A forced vibration results when an outside periodic force is applied to the object. This type of vibration is

not related to the object's location and motion. The vibration that results from a ball impacting a bat is an example of a forced vibration. A free vibration is one caused by gravitational or elastic forces that act on the body. They depend on the object's location and motion.

Forced and free vibrations can also be broken down into damped and undamped vibrations. An object has damped vibration when forces exist that resist the restoring force. A restoring force is a force that causes the object to return to its equilibrium position. In undamped vibrations, there are no forces that resist the restoring force. If there are such forces, they are very small, and therefore, negligible. Thus a bat is considered undamped. The hands do act as dampers and absorb most of the energy; however, the resisting forces are small and so these forces are negligible.

2.5.3 Deformation and Restoration

When a ball impacts a bat, a collision between two elastic bodies takes place. Upon impact, there is a change in velocity either in the ball, the bat, or in both the ball and the bat. Reaction forces cause deformations in the objects involved in the impact. The deformation causes mechanical energy to be converted into heat and sound.

When two bodies undergo a collision, there are two phases: deformation and restoration. During the deformation phase, interaction forces compress the objects. This phase lasts from the initial contact to the point of maximum deformation. The deformation phase ends when there is no velocity along the line of impact (Riley and Sturges, 1993). For example, the ball is not moving any closer to the bat and it is not

moving any further away from the bat. The same is true for the bat with respect to the ball. The amount of deformation depends on the material of the object, the temperature, and the rate of deformation (Riley and Sturges, 1993).

The restoration phase begins with the point of the object's maximum deformation. It ends when the two objects separate. The two bodies are pushed apart when each object's internal forces try to return the object to its initial form. In many cases, there is a small amount of permanent deformation. As a result of the deformation and the sound vibrations produced, some of the initial mechanical energy is lost (Riley and Sturges, 1993).

During the impact of two objects, linear momentum is conserved. However, if each object is studied separately, the internal forces are impulsive in the object and must be considered. The equation used for linear impulse-momentum in the deformation phase is

$$m_A v_{Ai} - \int_{t_i}^{t_c} F_d dt = m_A v_c$$

where m_A is the mass of object, $\int_{t_i}^{t_c} F_d dt$ represents the deformation impulse and F_d is the interaction force during the deformation phase, t_i and t_c are the beginning and ending times of the deformation phase, and v_c is the velocity of both objects at the end of the deformation phase (Riley and Sturges, 1993).

The linear impulse-momentum equation for the restoration phase is

$$m_A v_c - \int_{t_c}^{t_f} F_r dt = m_A v_{Af}$$

where $\int_{t_c}^{t_f} F_r dt$ represents the restoration impulse, F_r represents the interaction force during the restoration phase, t_f is the time at the end of the restoration phase, and v_{Af} is the final velocity of the object A after the impact (Riley and Sturges, 1993).

2.5.4 Coefficient of Restitution

The coefficient of restitution is the ratio of the deformation impulse to the restoration impulse. For object A, the coefficient of restitution is expressed as

$$e = \frac{\int_{t_c}^{t_f} F_r dt}{\int_{t_i}^{t_c} F_d dt} = \frac{m_A v_c - m_A v_{Af}}{m_A v_{Ai} - m_A v_c} = \frac{v_c - v_{Af}}{v_{Ai} - v_c}$$

where v_{Ai} and v_{Af} , are the initial and final velocity of object A, and v_c is an unknown velocity. For object B, the other object involved in a collision, the coefficient of restitution can be reduced to

$$e = \frac{v_{Bf} - v_c}{v_c - v_{Bi}}$$

where v_{Bi} and v_{Bf} are the initial and final velocities of object B, and v_c is an unknown velocity. If the unknown velocity is eliminated from the equations for the COR, coefficient of restitution, for objects A and B, and the equations are combined, then the resulting COR is

$$e = \frac{v_{Bf} - v_{Af}}{v_{Bi} - v_{Ai}}$$

(Riley and Sturges, 1993). The COR is the negative ratio of the speed of the two objects before and after the impact (Van Zandt 1991). It is also basically the measurement of the elasticity of an object. If COR is equivalent to one, then the impact is considered perfectly elastic. For a perfectly elastic impact, the energy in the impact is conserved. However, the COR is rarely equal to one, so for most impacts, energy is lost and the collision is not perfectly elastic (Riley and Sturges, 1993). For an impact between an aluminum bat and ball, a COR of 0.5 is fairly common. With a 0.5 value for the COR, approximately 24.5% of the impact energy will be returned to the bat and the ball (Adair, 1990). Since energy is lost during impact and the COR measures the elasticity of the objects, in a sense, the COR can also be said to measure lost energy (Hester and Koenig, 1993).

In a collision between a bat and ball, the ball can be represented by object A and the bat can be represented by object B. The COR measures the elasticity of these two objects or in other words, the amount of energy lost in the impact. Most of this lost energy remains in the bat in the form of vibration.

2.5.5 Impact

When a ball impacts a bat, it is not a perfectly elastic collision. Energy is lost. However, when the ball strikes the bat at a node (a point of no deflection), the impact is more elastic. In this situation, the aluminum bat has more elasticity than the ball. A wooden bat would not be as stiff. If the impact is highly elastic, about one-eleventh of the impact energy is stored in the bat's deformation. This stored energy is then returned

to the ball. When the ball deforms, about ten-elevenths of the impact energy was stored in the deformation. Unfortunately, most of this energy is lost (Adair, 1990).

Approximately 80% of the bat's deformation energy is transferred to the ball. The remaining energy that is not transferred to the ball is retained in the energy of motion of the bat's aluminum shell (Adair, 1990).

2.5.6 Frequency

When something vibrates there is a frequency of oscillation. The frequency is defined as

$$f = \frac{1}{\tau}$$

where τ represents the period. The period of oscillation is the time it takes the motion of vibration to repeat. Frequency is measured in cycles per second. A typical frequency plot can be seen in Figure 2.

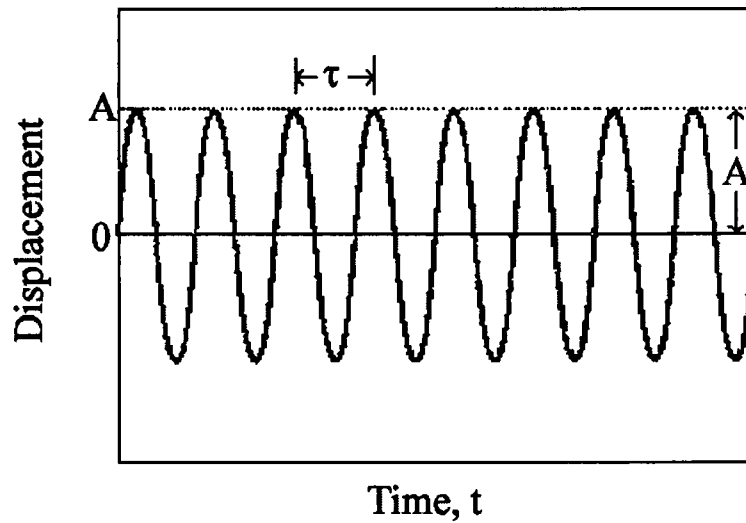


Figure 2: Frequency Plot (Riley and Sturges, 1993).

The period, τ , and the frequency mode of oscillation and the amplitude of the oscillation are shown in the plot.

2.5.7 Natural Frequencies

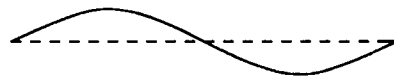
There are different modes of vibration. A mode is simply, in layman's terms, the shape of the vibration. An example of the first two modes for a cantilever beam with both ends free, one clamped end and one free end, and both ends clamped are illustrated in Figures 3 – 5 respectively.



Simple Beam
Free Ends



First Mode

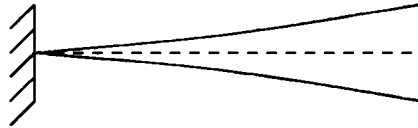


Second Mode

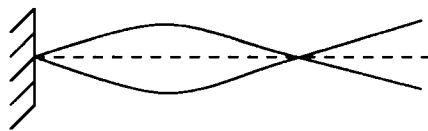
Figure 3: First two modes for a free-free beam.



One End Clamped and the Other Free



First Mode



Second Mode

Figure 4: First two modes for a cantilever beam with one end clamped and one end free.

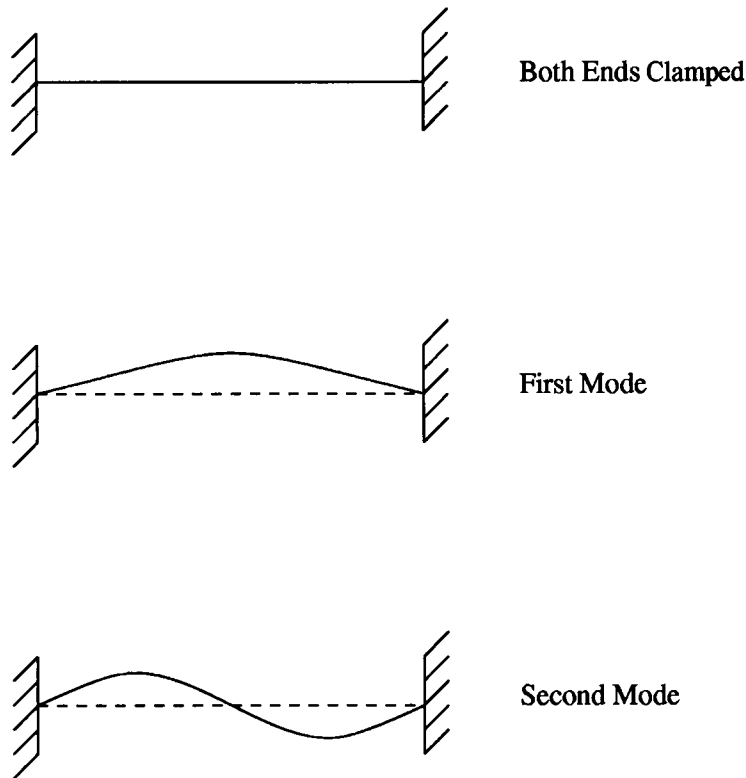


Figure 5: First two modes for a fixed-fixed beam with both ends clamped.

For a thin walled cylinder there are two types of modes: beam and shell. The beam mode of an object will change if there is a change in the structure, mass, or stiffness of the object. The shell mode changes are related to the thickness and span distribution of the object. The amplitude of oscillation is the maximum displacement of the object from its initial equilibrium position.

For shell modes, the length of the span affects the mode of vibration. If, in Figure 6, L_1 represents the long span, and, if the span of the beam shortens to L_2 , then the result is a new mode of frequency. The frequency of vibration depends on the modes that have

been excited. Since shell modes depend upon the length of the beam, the first mode of a shorter span could be lower in frequency than the second mode of a longer span.

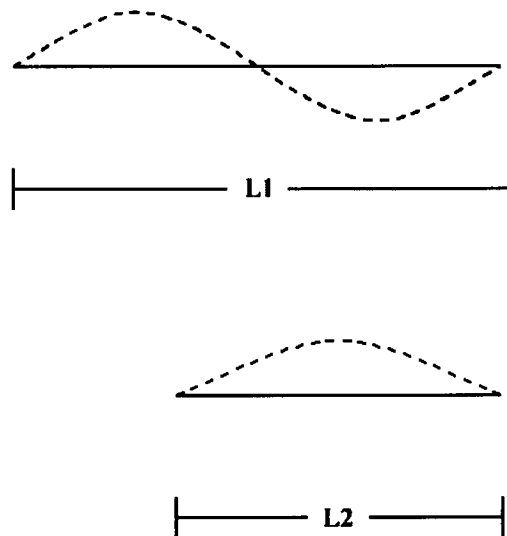


Figure 6: Effect of span length on mode of vibration. L1 represents the length of the original span and its corresponding mode of vibration. L2 represents the shorter span with a different mode of vibration.

2.5.8 Antinodes and Nodes

The jarring sensation felt in the handle of the bat is the direct result of a ball striking the bat “on an antinode of the bat’s transverse vibration” (Kirkpatrick, 1962). (In other words, hitting the bat on a point other than at the sweet spot.) When the bat is struck at a location other than a sweet spot, only part of the energy is transferred back into the ball after the impact (Kirkpatrick, 1962). An antinode is the point of maximum deflection in the mode of vibration. For example, in the first mode of vibration of the bat’s natural frequency, the antinode is located in the middle of the mode. When a rubber

band is stretched and then pulled it vibrates, or oscillates, back and forth about its initial equilibrium position. The maximum point of deflection in this oscillation is the antinode. A node is a point of no deflection, so for the stretched string example, there would be two nodes, one at each end where the rubber band is held. Antinodes and nodes can be seen in Figure 7.

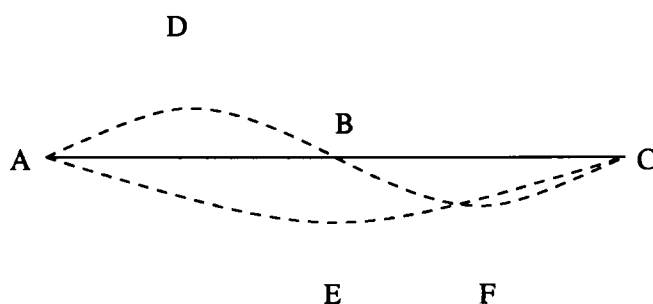


Figure 7: Antinodes and nodes. The nodes are represented by A, B, and C. The antinodes are represented by D, E, and F.

2.5.9 Sting of the Bat

In past studies it has been determined that hitting the bat on an antinode should be avoided because a broken bat is sometimes the result (Kirkpatrick, 1962). When the ball does not hit the sweet spot, the energy of distortion is not returned to the ball from the bat; instead, it remains in the bat in a form of vibration (Adair, 1990). By striking an antinode on the bat, useful kinetic energy is diverted into vibrational motion (Kirkpatrick,

1962). The vibration that is felt in the handle is often referred to as the sting of the bat. According to the Law of Conservation of Energy, “the more energy transmitted into the bat (and not reflected into the ball), the more energy is transmitted into the hitter’s hand” (Dunbar and Toganarelli, 1994).

Within milliseconds after the ball hits the bat at an antinode, the vibration travels from the point of impact down through the handle and into the hitter’s hands. “As the impulse passes into the handle, its amplitude grows, and the handle whips forward” (Dunbar and Tognarelli, 1994). If the ball hits the bat on the barrel side of the center of percussion then the handle will slap a right-handed hitter’s left palm. When the ball impacts the bat on the handle side of the center of percussion, then the handle will slap a right handed hitter’s right palm (Adair, 1990). This takes place within approximately 2.5 milliseconds after the initial impact of the bat and ball. The bat whips back between 4 and 5 milliseconds. The hitter’s hands absorb the energy from the handle; they act as dampers and damp the motion of the bat (Dunbar and Tognarelli 1994).

2.5.10 Testing Handle Vibration

Many tests have been performed in order to study the handle vibration. One method used for testing was to impact bats at different locations while someone held the handle of the bat. The pain caused from the sting of the bat was then measured. Results from this type of analysis can be seen in Figure 8 (Noble and Walker 1994).

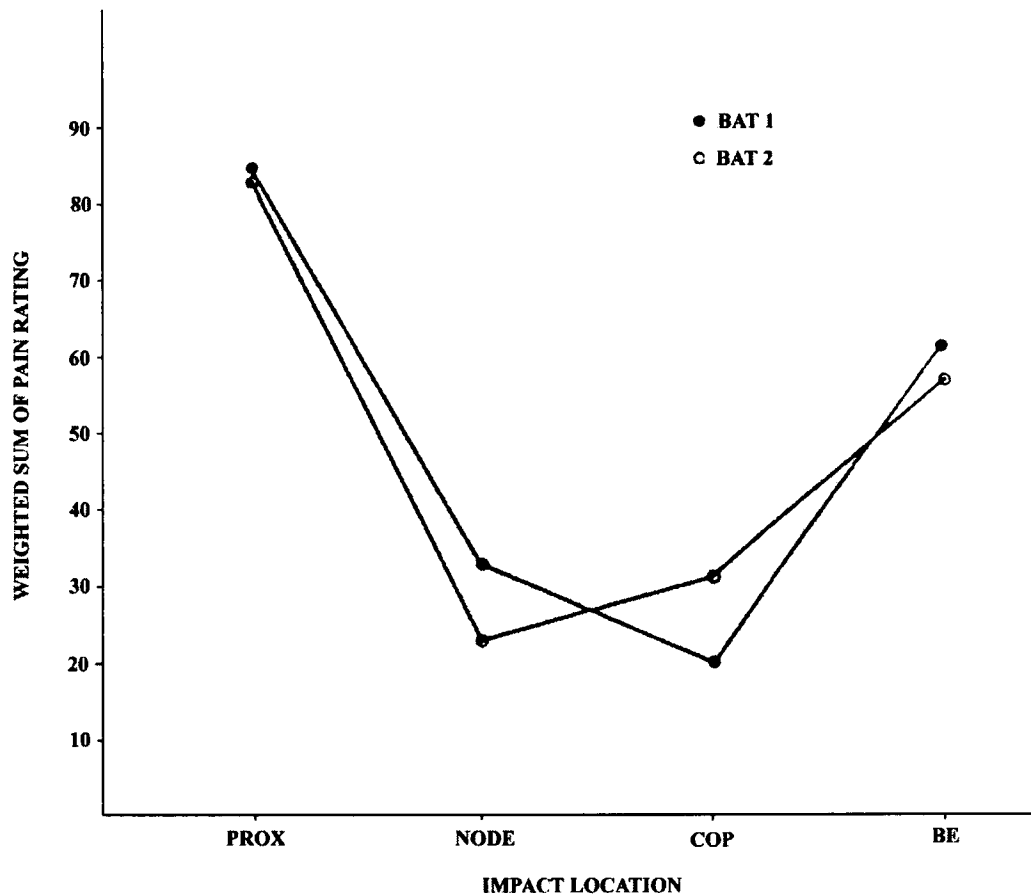


Figure 8: Pain ratings caused from the sting of the bat. Impact locations on the bat were center of percussion (COP), node of the fundamental mode of vibration (NODE), near the end of the barrel (BE), and two inches from the center of percussion on the handle end (PROX). Bat 1 and bat 2 were different sized bats (Noble and Walker, 1994).

Two different sized bats were impacted at the center of percussion (COP), node of fundamental mode of vibration, near the barrel end (BE), and near the handle (PROX). Bat 1 was slightly larger than bat 2. Bat 1 was 23% heavier and 3% longer than bat 2. Its frequency was also 19% higher. The center of percussion for bat 1 was 5% closer to the axis than the center of percussion for bat 2. The axis is usually located at the point where the hands grip the bat. The axis is the point where the “impact reaction torques are

equally distributed” (Noble, 1983). The proximal node for the fundamental frequency was 2 centimeters closer to the knob on the handle on bat 1 than on bat 2. The two bats were impacted by a baseball travelling at 60 mph. The analysis began 5 milliseconds before the ball/bat impact and continued until no vibration remained. The total time was 0.4 seconds. A weighted sum was used to rate the pain: 0 = no pain, 1 = slight pain, 3 = moderate pain, and 5 = severe pain. From Figure 8, it is easily seen that less pain is felt when the ball impacts the bat at the node or the center of percussion.

Past studies have shown that when a ball impacts a bat at an antinode, energy is lost and vibration results. It was also stated that the antinode is the point of maximum deflection. Objects when impacted deflect and interaction forces then restore the objects back to their initial form. Since an antinode is a point of greatest deflection and both bat and ball deform upon impact, a theory has been established stating that a ball will travel further if it impacts the bat on an antinode of the first or second mode. However, for this theory to be successful, timing is of vital importance.

2.5.11 Ball and Bat Deformation

When a ball impacts the bat, both ball and bat deform. Recent studies have shown that a ball will deform to almost one half of its original size when it impacts a bat. The bat will deform one tenth as much as the ball (Adair, 1990). A simplified representation of the cross section of a ball, as it impacts a bat, can be seen in Figure 9. The different velocities represent ball velocity as it impacts the bat. In reality, in a ball

and bat collision, the ball will deform more on the side of impact. The side of impact on the ball will flatten.

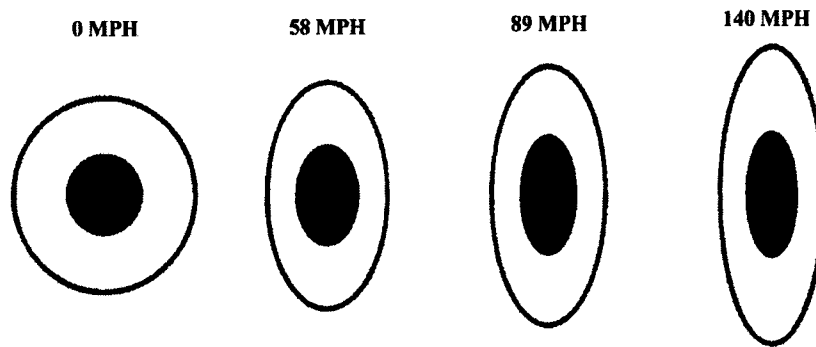


Figure 9: Cross section of ball as it impacts bat at different velocities (Adair, 1990).

2.5.12 Trampoline Effect

After maximum deformation has occurred, internal forces in the bat and the ball begin restoring them back to their original forms. For the ball to achieve maximum velocity and distance, both bat and ball must begin and end the restoration phase at the same instant. When the bat snaps back to its original shape, all the energy is transferred into the ball. It is a trampoline effect. A model, of a ball impacting a section of a bat with a trampoline effect, can be seen in Figure 10. When jumping on a trampoline, a person bends their legs as they make contact with the trampoline, and then the legs are extended as the person is catapulted back into the air. Maximum height will be achieved if at the instant the trampoline is springing back, the person is extending their legs. However, if the person extends their legs before the trampoline springs back, they will

not be catapulted very high. This is based on the timing of the deformation and restoration phase. In order for there to be maximum height and distance, the phases must be equal in their lengths. This is also what has to happen to get maximum ball flight distance when the ball leaves the bat after the ball has impacted an antinode on the bat. If for example, the restoration phase of the ball begins while the bat is still in the

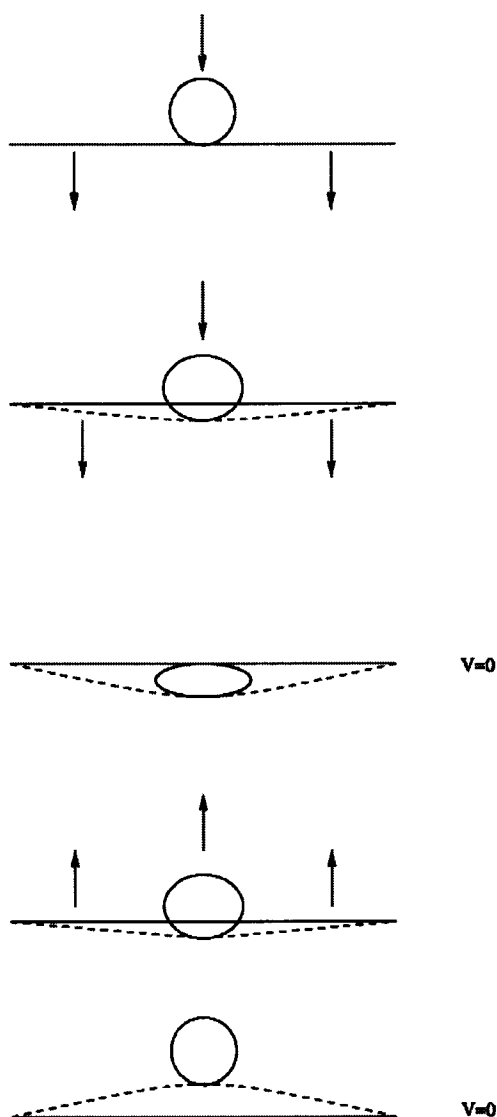


Figure 10: Trampoline effect occurring when ball impacts a bat.

deformation phase, there will be a loss of energy. The ball will already be leaving the bat before the bat snaps back. When this happens, an antinode is not the ideal place to hit the bat: but, if the deformation and restoration of the bat and ball are equal in time then impacting the bat at an antinode is an ideal location. Also, when this occurs, the COR will be equal to one and the impact is perfectly elastic, no energy is lost.

2.6 CLAMPED VERSUS UNCLAMPED

When designing a new bat, it is important to use models of bats for the dynamic analysis. It must first be determined whether a bat that was clamped at the handle or unclamped best represent a hand held bat. In past studies, both clamped and unclamped bats were analyzed. It was determined that an unclamped bat best modeled a hand held bat.

2.6.2 Normal Mode and Modes of Oscillation

A normal mode is the free vibration of an elastic system. When studying the “elastic behavior of a bat under ball impact conditions,” the first twenty normal modes are sufficient (Van Zandt, 1991). The normal modes of a bat are “analogous to the harmonics of a stretched string;” however, with a bat, the overtones are not harmonic (Van Zandt, 1991). The normal modes of oscillation, for a clamped bat and an unclamped bat, are very different (Noble and Walker, 1994). The lowest modes of oscillations for a clamped and unclamped bat can be seen in Figure 11.

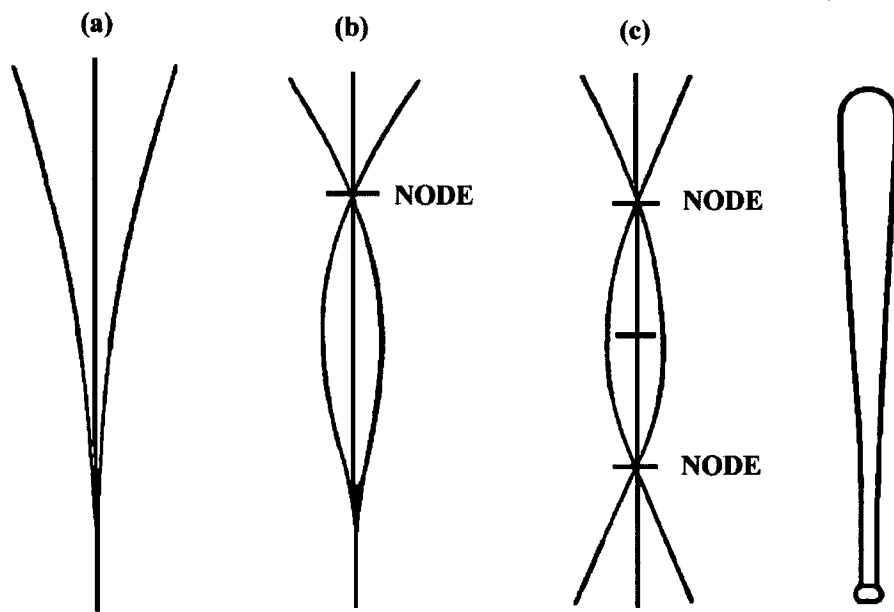


Figure 11: Bat's lowest modes of oscillation: fundamental mode for a clamped bat also called the diving board mode (a), 2nd mode of oscillation for a clamped bat (b), and lowest frequency of oscillation for a bat with free ends (c) (Brody, 1989).

The clamped bat's fundamental mode of oscillation is the diving board mode. For this type of mode, the node is located at the point where the bat is clamped, usually near the handle. The clamped bat's "next higher mode of oscillation" also has the node at the clamp as well as a node past the bat's center of mass. This is called the first harmonic mode (Noble and Walker, 1994).

The normal modes of oscillation for a free or unclamped bat vary from those of the clamped bat. Whereas, the first mode of frequency for a clamped bat has one node, a free bat has two. These are located approximately "twenty percent of the bat length from each end" (Noble and Walker, 1994). The free bat's lowest frequency of oscillation also has "a period not greatly different from the period of the first harmonic of a clamped bat,

and an outer node that is located near the position of the node of the first harmonic of the clamped bat” (Brody, 1989).

When a clamped bat is hit near the tip of the barrel away from the node, the diving board mode and the first harmonic mode are present. When the free bat is struck in the same manner at the tip, the first harmonic mode, two-node mode, is the lowest frequency observed. This off node hit has a twenty- percent lower frequency of oscillation than the clamped bat’s higher frequency oscillations. Figure 12 shows that the higher frequency oscillations of a free bat damp out quicker than the lower frequency oscillations of a clamped bat. The diving board mode is not present in the free bat’s oscillations because this low mode of vibration is not excited (Brody, 1989).

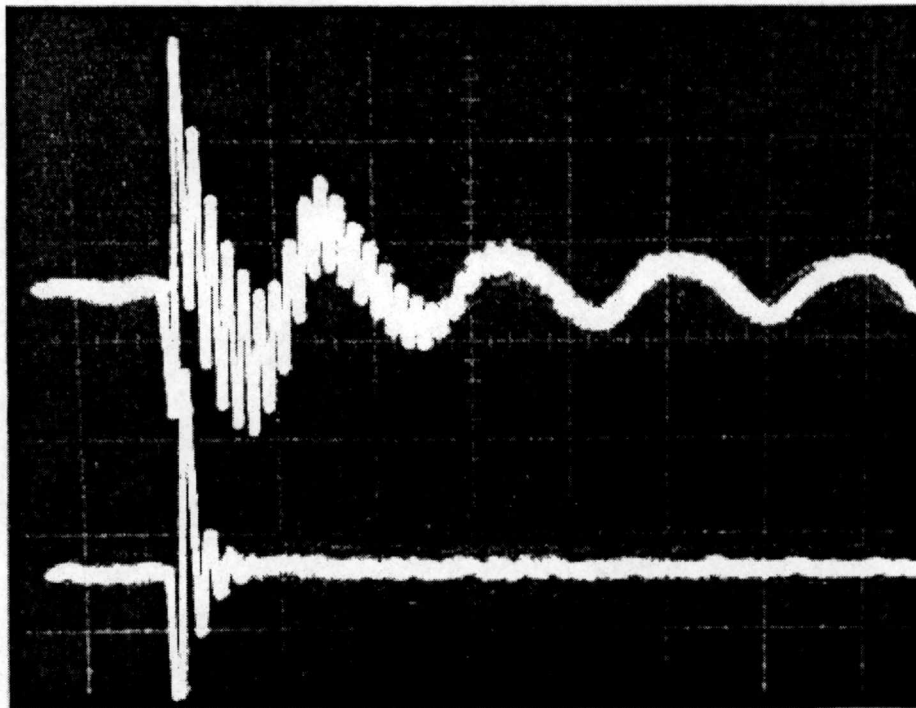


Figure 12: Oscilloscope traces showing vibration of a bat with its handle clamped in a vise (upper trace) and a bat that is hand held (lower trace) (Brody, 1989).

For a clamped softball bat, the frequency of the lowest mode of vibration is approximately equal to 27 Hz. The unclamped softball bat has its lowest frequency equal to approximately 163 Hz. This is a simple bending mode (Van Zandt, 1991).

When a bat is hit near a node, then the bat would have a lower amplitude in the frequency of oscillation than if it were an off node hit, or antinode. Hitting the bat near an antinode causes much higher amplitude in the frequency oscillations. A bat hit near a node does not have the higher frequency oscillations, only lower frequency oscillations are present. This can be seen in Figure 13 (Brody, 1989).

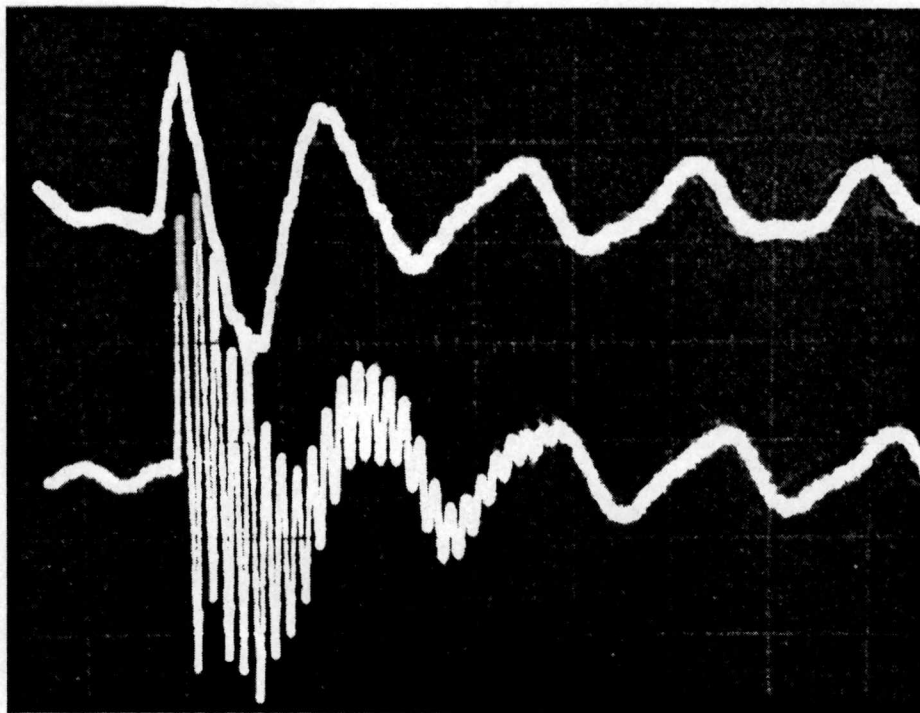


Figure 13: Oscilloscope traces showing the vibration of a bat with its handle clamped in a vise. The impact was near the node (upper trace) and near the tip (lower trace) (Brody, 1989).

There are no low frequency oscillations when a hand held bat is hit near a node or even an antinode. This demonstrates that a hand-held bat acts like a free or unclamped bat, since free bats do not have the low frequency oscillations (Brody, 1989). The low frequency oscillations in the clamped bats occur because there is a “greater mass to swing about a correspondingly larger moment arm” (Van Zandt, 1991). On a hand held bat, the hands act as dampers. They absorb some of the vibration that occurs when the bat is struck at an antinode (Brody, 1989).

2.6.3 Distance and Vibration

The distance a ball travels after impact and the study of bat vibration has no bearing on whether the bat is clamped or unclamped. When a ball impacts a bat, it is only in contact with the bat for about 0.001 of a second. The point of contact on the bat only moves about an inch during this small fraction of time. The bat’s handle moves even less. If the bat is impacted near the center of percussion and there is minimal movement at the handle during the impact, then the bat can be treated as a free body and all clamping effects are irrelevant (Adair, 1990). Therefore, it is not necessary to assume that the bat is free and unclamped at the handle (Van Zandt, 1991).

2.6.4 Handle Grip

The grip a player has on the bat can also be compared to whether the bat is clamped or unclamped at the handle. The grip can be considered a boundary condition at the handle. Since a ball is only in contact with the bat for a fraction of a second, it

doesn't matter whether the bat is tightly gripped or not. In fact, if the bat was released at the exact moment of impact and radial velocity is assumed to be zero, there would be no effect on the velocity of the ball. The ball would still have the same trajectory as if the bat had been gripped firmly throughout the swing. Once again, it has been shown that the handle's boundary conditions are irrelevant (Van Zandt 1992).

The amount of grip does, however, affect the duration of the vibration. The hands act like dampers. The vibration felt in a tightly gripped bat will damp out quicker than the vibration in a loosely gripped bat (Brody, 1989). The hands absorb some of the shock.

2.7 IMPACT ENERGY TEST

An impact energy test can be used to study the effect of impacting the sweet spot and how this affects the amount of vibration felt in the handle. The drop tower test is a type of impact energy test that has been used in the past for evaluating softball and baseball bats. The drop tower test "puts a controlled energy input into the component under test and then measures how much energy was absorbed by the component" (Dunbar and Tognarelli, 1994). This test allows the tester to see how much energy is transferred into the ball from the bat.

Dunbar and Tognarelli conducted drop tower tests where an impact energy level of 2 ft-lb at a velocity of 4.61 ft/sec was input into the bat. The location of the impact varied from 2 - 7 inches from the barrel end of the bat. For the bat tested, a sweet spot

was located at approximately 5 inches from the barrel end. The results of this test can be seen in Figures 14 - 19 (Dunbar and Tognarelli, 1994).

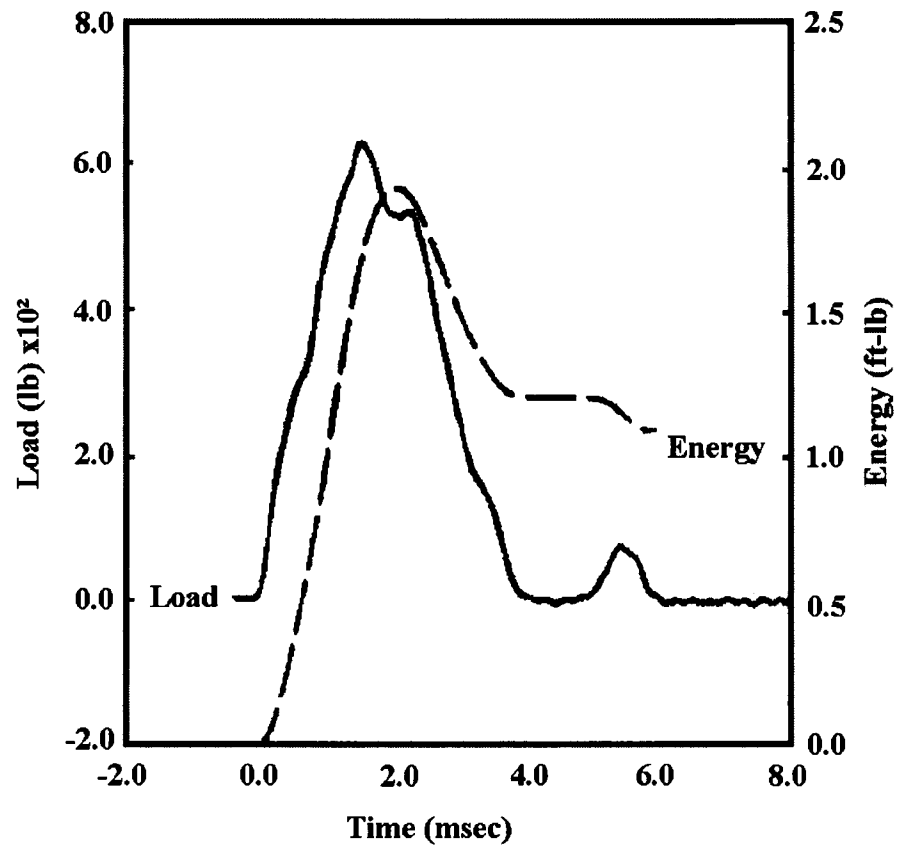


Figure 14: Load and energy curves with respect to time for a bat impacted 2 inches from the barrel end (Dunbar and Tognarelli, 1994).

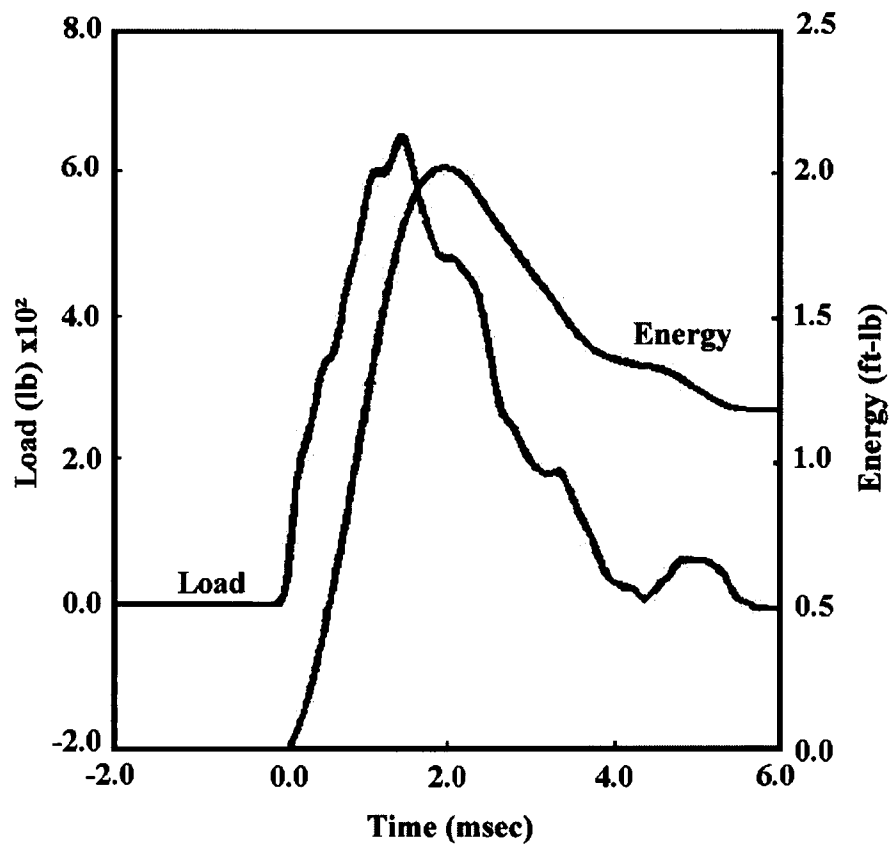


Figure 15: Load and energy curves with respect to time for a bat impacted 3 inches from the barrel end (Dunbar and Tognarelli, 1994).

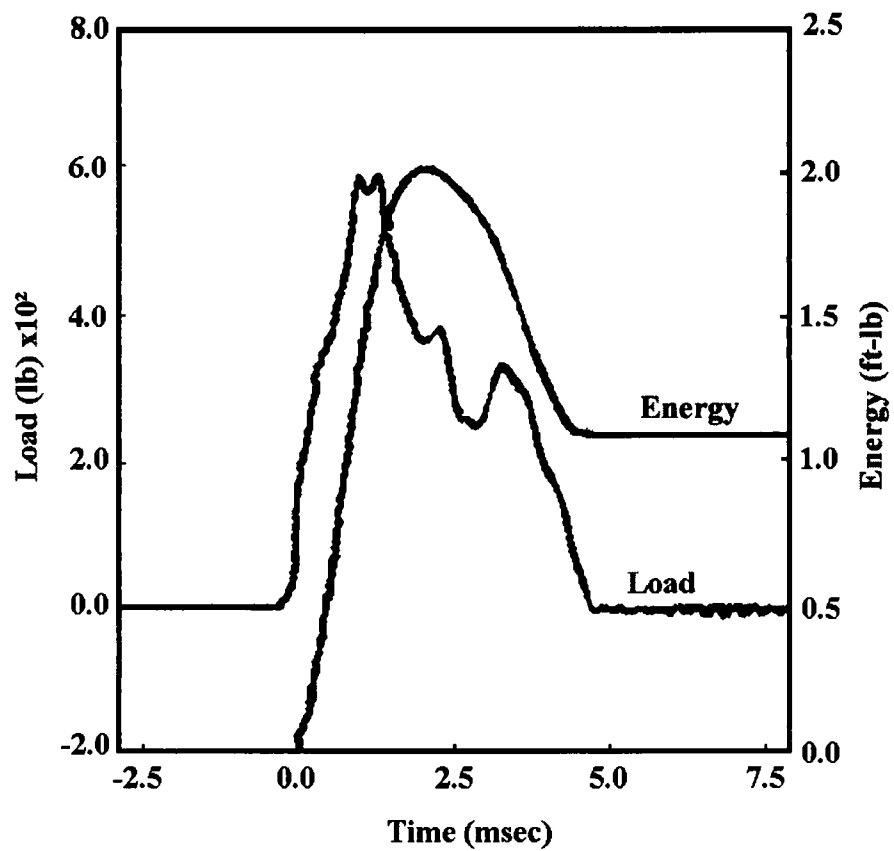


Figure 16: Load and energy curves with respect to time for a bat impacted 4 inches from the barrel end (Dunbar and Tognarelli, 1994).

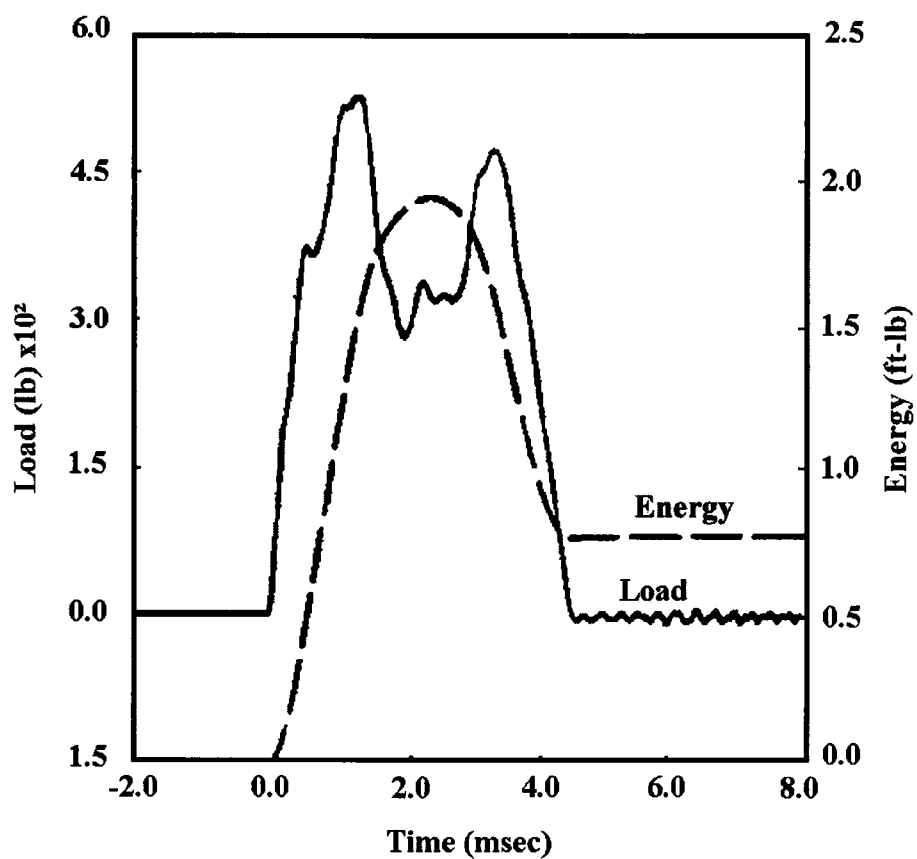


Figure 17: Load and energy curves with respect to time for a bat impacted 5 inches from the barrel end (Dunbar and Tognarelli, 1994).

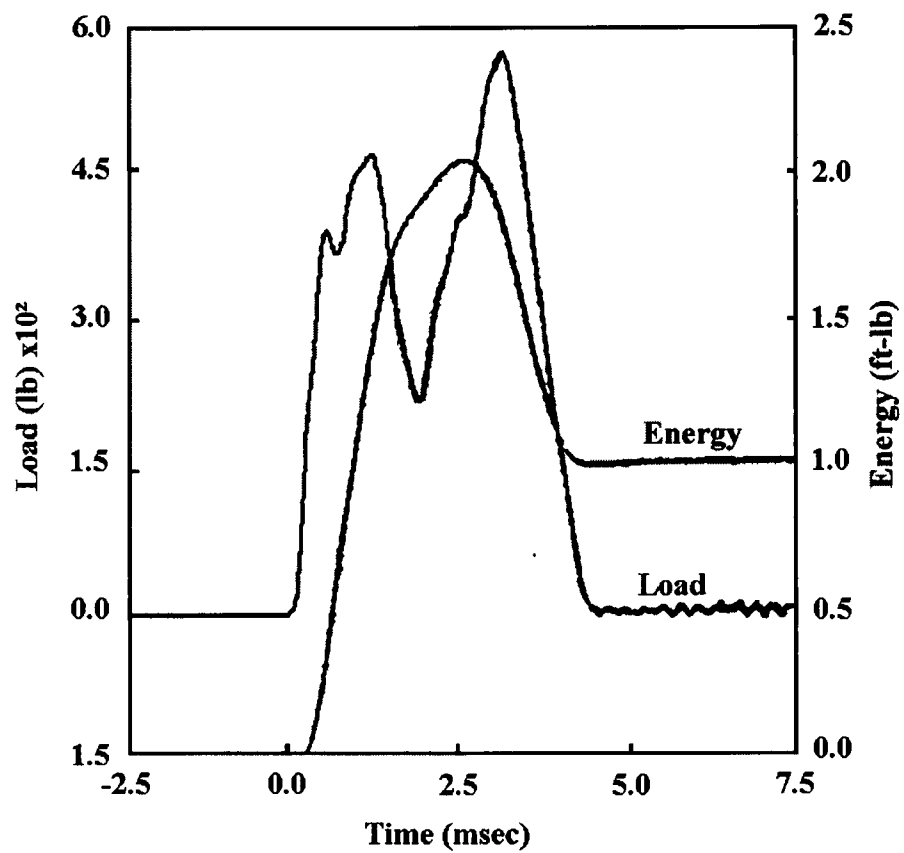


Figure 18: Load and energy curves with respect to time for a bat impacted 6 inches from the barrel end (Dunbar and Tognarelli, 1994).

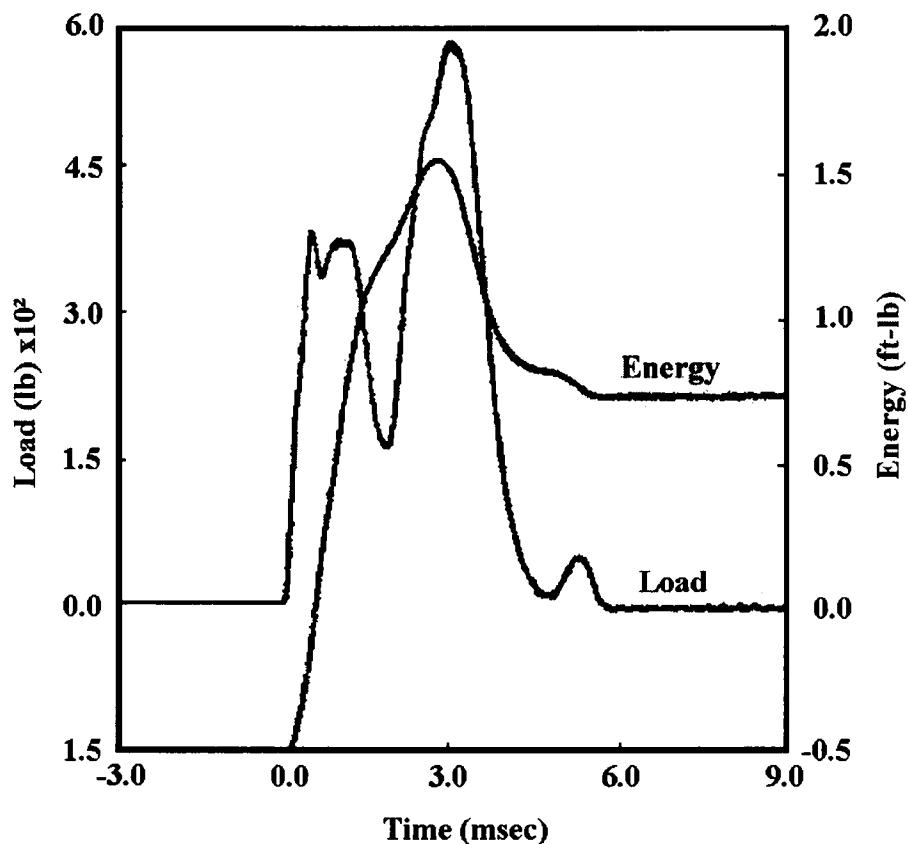


Figure 19: Load and energy curves with respect to time for a bat impacted 7 inches from the barrel end (Dunbar and Tognarelli, 1994).

From Figure 17, it can readily be seen that at 5 inches from the end (the sweet spot) “maximum energy is transferred from the bat to the ball” (Dunbar and Tognarelli, 1994). This graph shows that less energy remains in the bat after impact. This graphically shows why less handle vibration is felt when the bat is impacted in a sweet spot zone. Since more energy is transferred into the ball instead of the handle, the ball will go farther. The graphs also show that more handle vibration occurs when the bat is impacted at the barrel end (Dunbar and Tognarelli, 1994).

2.8 SUMMARY OF REVIEWS

Baseball and softball bats have come a long way over the years. They are continuously being optimized. Once bats were only made from wood, but today's bats are made from lightweight, durable aluminum as well as wood. The aluminum bats of today are much lighter and more flexible than the bats of yesteryears.

When optimizing a bat, the sweet spot is the main focus of concern. When a ball strikes the sweet spot on the bat, the ball will travel farther and less vibration will be felt in the handle of the bat. Decreasing this handle vibration is of great importance when optimizing the performance of a bat.

To study the vibration and the location of the sweet spot, the bat must first be modeled. An unclamped bat best models a hand - held bat; however, the fact that a bat handle is clamped or unclamped is not related to the results.

A method that was used in the past to study the affects of a ball striking a bat at a sweet spot and handle vibration in the bat was the impact energy test. From this test it was seen that a ball will travel farther and there will be less handle vibration when the ball strikes the bat at one of the sweet spots. Therefore, to obtain a better performance bat, it is necessary to increase the size of the sweet spot.

3. COSMOS

3.1 INTRODUCTION

“COSMOS/M is a complete, modular, self-contained finite element system developed by Structural Research and Analysis Corporation for personal computers and workstations” (Ali and Traina, 1993). The COSMOS/M program can be used to “solve linear and nonlinear static and dynamic structural problems, in addition to solving problems in the fields of heat transfer, fluid mechanics, electromagnetics and structural optimization” (Ali and Traina, 1993). “The COSMOS/M system consists of a pre- and postprocessor, various analysis modules, interfaces, translators and utilities. The program is completely modular allowing the user to acquire and load only the modules that are needed” (Ali and Traina, 1993).” For this project, a Silicon Graphics Indigo 2 workstation was used.

3.2 GEOSTAR

“GEOSTAR is the basic pre- and postprocessor of the COSMOS/M finite element system. It is an interactive full three-dimensional CAD-like graphic geometric modeler, mesh generator and FEA pre- and postprocessor” (Ali and Traina, 1993). It is the core of the system. GEOSTAR can be used to create a model with proper geometry, mesh the model, and subject the model to an analysis. When analyzing the model, the system exits GEOSTAR and connects to the analysis module. “The GEOSTAR program controls the execution of the various analysis modules of the COSMOS/M package and

provides an interaction environment among them” (Ali and Train, 1993). Once the analysis is completed, the system then reenters GEOSTAR for plotting and printing the results. There are many different types of analysis modules in the program. STAR for linear static analysis; DSTAR for buckling, frequency, and mode shape analysis; and ASTAR for advanced dynamic linear analysis, were used in this project. (Ali and Traina, 1996).

3.3 STAR

The STAR module performs a linear static analysis on the model being studied. Structural deformations of the model are calculated in the STAR module by using the linear theory of structures, which is based on small displacement assumptions. The displacement method uses the following equation to solve linear static problems:

$$[K]\{U\} = \{F\} = \{F^a\} + \{F^c\}$$

In this equation $[K]$ represents structural stiffness matrix, $\{U\}$ is equivalent to the vector of the unknown nodal displacements, and $\{F\}$ represents the load vector which can be represented by a combination of applied nodal loads, $\{F^a\}$, and reaction forces, $\{F^c\}$. In linear static problem, $\{F^a\}$ and $\{F^c\}$ are the sums of the mechanical, thermal and gravitational loads. $\{F^m\}$ is the mechanical load vector. The following equation can be used to calculate the mechanical load vector, $\{F^m\}$:

$$\{F^m\} = \{F^{nd}\} + \sum_{e=1}^{nel} \{F_e^{pr}\}$$

where $\{F^{nd}\}$ represents the applied nodal load vector and $\{F_e^{pr}\}$ is equivalent to element load pressure. The thermal load vector, $\{F^{th}\}$, can be determined by using

$$\{F^{th}\} = \{F^{nt}\} + \sum_{e=1}^{nel} \{F_e^{th}\}$$

where $\{F^{nt}\}$ represents the nodal temperature load vector and $\{F_e^{th}\}$ represents the element thermal load vector. The gravitational load vector is calculated by using

$$\{F^{gr}\} = \left(\sum_{e=1}^{nel} [M_e] \right) \{a\}$$

where the element mass matrix is represented by $[M_e]$ and $\{a\}$ represents the acceleration vector (Ali and Traina, 1996).

A partitioned structural stiffness matrix is used to describe the model's behavior when forces and fixed and/or prescribed motions are applied to it. The partitioned structural stiffness matrix used by COSMOS/M is as follows:

$$\begin{bmatrix} [K_{ff}] & [K_{fs}] \\ [K_{sf}] & [K_{ss}] \end{bmatrix} \begin{Bmatrix} \{U_f\} \\ \{U_s\} \end{Bmatrix} = \begin{Bmatrix} \{F_f^a\} \\ \{F_s^a\} \end{Bmatrix} + \begin{Bmatrix} \{0\} \\ \{F_s^c\} \end{Bmatrix}$$

where the degrees of freedom are represented by the subscript f and the subscript s are equivalent to the degrees of freedom that have specified values (Ali and Traina, 1996).

A linear relationship of displacements exists between two or more nodes. This can be specified by constraint or coupling equations. The constraint equations are a way of modeling dependent degrees of freedom. Dependent degrees of freedom are the "linear combinations of one or more other degrees of freedom" (Ali and Traina, 1996).

The constraint equations in COSMOS/M only use the degrees of freedom chosen. The constraint equation can be expressed as

$$\{U_m\} = [C_m]\{U_n\}$$

where the vector of dependent degrees of freedom is represented by $\{U_m\}$, the independent degrees of freedom are represented by $\{U_n\}$, and the constraint equation matrix is represented by $[C_m]$. After both sides of the displacement method equation are partitioned for independent and dependent degrees of freedom, the constraint equations are applied. Before $\{U_m\}$ can be eliminated, the constraint forces have to be added to the displacement method equation (Ali and Traina, 1996).

3.4 DSTAR

During this research, the DSTAR module was used to calculate the bat's natural frequencies and the corresponding mode shapes. This analysis, performed by DSTAR, is called a modal or normal mode analysis. Buckling loads can also be calculated by using the DSTAR module (Ali and Traina, 1996).

3.4.2 Normal Mode Analysis

For dynamic systems, the finite element system of equations used is

$$[K]\{U\} + [C]\{\dot{U}\} + [M]\{\ddot{U}\} = \{F(t)\},$$

where $[M]$ represents the mass matrix, and the damping matrix is represented by $[C]$.

When there is free vibration in the system,

$$[K]\{U\} + [C]\{\dot{U}\} + [M]\{\ddot{U}\} = \{0\}$$

is the form of finite element system of equations used (Ali and Traina, 1996).

The equation used for undamped linear elastic structures is

$$[K]\{U\} + [M]\{\ddot{U}\} = \{0\} .$$

When there is an initial displacement of a linear elastic system that has no damping, the system will indefinitely oscillate. The oscillations will have the same mode shapes but the amplitudes will vary. The term mode shape is used to describe the shapes of the oscillations. A natural frequency is the frequencies of these mode shapes (Ali and Traina, 1996).

If the system has no external loads acting upon it, then it is assumed that the system would freely vibrate harmonically. This harmonic form is expressed by

$$U(t) = \phi \sin(\omega t + \theta).$$

This harmonic equation leads to the eigenvalue problem

$$[[K] - \omega^2 [M]]\{\phi\} = \{0\}$$

where the natural frequency is represented by ω and ϕ is the systems mode shape (Ali and Traina, 1996).

An eigenpair extraction method is used for the frequency analysis. Subspace iteration, Lanczos, Jacobi, and inverse power iteration are methods that can be used to calculate the eigenvalues (Ali and Traina, 1996). The subspace iteration method was used for the research on the bat studied in this project.

3.4.3 Subspace Iteration

Subspace iteration is a type of eigenpair extraction method. It is often used when there is a large number of eigenvalues in the system of equations. Subspace iteration chooses an initial set of mode shapes. These mode shapes are usually representative of the structure's modes. The modes are then arranged in columns in a $n \times m$ matrix, Φ_1 , where n represents the order of the eigenvalue problem and m represents the number of modes. The number of modes chosen should be much smaller than the order of the problem (Ali and Traina, 1996).

Once the matrix, Φ_1 , is formed, the equation

$$[K]_{n \times n} [T_h]_{n \times m} = [M]_{n \times n} [\Phi_1]_{n \times m},$$

is solved for T_h where $h = 2$. The equations:

$$K_{(m \times m)}^{(h)} = T_h^T K T_h \quad \text{and}$$

$$M_{(m \times m)}^{(h)} = T_h^T M T_h$$

are formed.

Next, the eigenvalues and eigenvectors of the system,

$$K^{(h)} V_h = M^{(h)} V_h \Lambda_h,$$

are then solved by an iterative technique such as the Jacobi iteration method. The result after solving the system is an improved set of eigenvectors:

$$\Phi_h = T_h^T V_h.$$

This process is repeated using the same equations with $h = h + 1$ until the system converges (Ali and Traina, 1996).

3.4.4 Jacobi Method

The Jacobi method is an iterative technique used to solve linear systems, such as $Ax = b$, where an initial approximation, $x^{(0)}$, for the solution x , has been made. A sequence of vectors, $\{x^{(k)}\}_{k=0}^{\infty}$, that converges to x is generated. The Jacobi method solves for x by using the following equation:

$$x_i^k = \frac{\sum_{\substack{j=1 \\ j \neq i}}^n (-a_{ij}x_j^{(k-1)}) + b_i}{a_{ii}}$$

for $i = 1, 2, \dots, n$ where n represents the number of unknowns and $k \geq 1$ (Burden and Faires, 1993).

3.5 ASTAR

The results obtained from the DSTAR calculations and the normal mode superposition method are used in the ASTAR, Advanced Dynamic Analysis Module, to calculate a structure's dynamic response. In the ASTAR module, several different types of analysis can be performed. The types include a modal time history, uniform and multi-base motion, frequency response, shock spectra, response spectra generation, random vibration, steady-state harmonic analysis, and PSD/Random response (Ali and Traina, 1993). A modal time history was used for the research performed on the bat.

3.5.2 Time History Analysis

When performing a time history analysis, “equations of motion for multidegree-of-freedom systems are solved subject to different dynamic loadings or base excitation functions” (Ali and Traina, 1993). Uncoupled equations of motion are first obtained by using a normal mode analysis. The motion for a linear dynamic system is determined by:

$$[M]\{\ddot{u}\} + [C]\{\dot{u}\} + [K]\{u\} = \{f(t)\}$$

where $[M]\{\ddot{u}\}$ equals the mass matrix times the displacement vector, $[C]\{\dot{u}\}$ equals the damping matrix times the velocity vector, $[K]\{u\}$ equals the stiffness matrix times the acceleration vector, and $\{f(t)\}$ equals the time varying load vector. This equation can then be decoupled into a single degree of freedom equation. This equation is written in “terms of the modal displacement vector $\{x\}$, where

$$\{u\} = [I]\{x\}$$

and $[I]$ is the matrix of the lowest eigenvectors” (Ali and Traina, 1993). This is the result of

$$[K]\{u\} = \omega^2 [M]\{u\} .$$

These equations are used to derive the following single degree of freedom uncoupled equation of motion:

$$x_i + 2\xi_i \omega_i x_i + \omega_i^2 x_i = \{\phi\}_i^T \{f(t)\} .$$

Once the uncoupled equations of motion are obtained, the response of each mode is then evaluated by using either the Wilson or Newmark method of step-by-step integration.

This type of integration solves the equations by using the results from each previous step

to obtain the results for the next step. The integration uses a time step increment, which means that the integration starts with the time from the previous step and concludes with the time at the current step. The solution's accuracy can be improved by decreasing the size of the time step increment between consecutive steps in the integration process. The transformation,

$$\{u\} = [\Phi]^T \{x\} ,$$

is then used at each time step to find the system's response (Ali and Traina, 1993).

In a time history analysis, the accuracy of the solution depends on three things: the number of modes used, accuracy in the modeling, and size of time step. The solution's accuracy can be improved by decreasing the size of the time step increment between consecutive steps in the integration process. It is recommended that a time step smaller than 1/10th of the period of the last mode be used (Ali and Traina, 1993).

4. PROCEDURE

4.1 INTRODUCTION

When using a finite element program such as COSMOS/M, a model of the system being studied has to be constructed. Three main steps were performed when designing the model of the bat that would be used in the analysis. First, the bat was drawn using the cad-like features of COSMOS/M. The next step in constructing the model was to mesh the bat. The third step in constructing the model was to choose the bat's material properties and real constants. Once these three steps were completed, the analysis could be performed.

4.2 DRAWING

The cad features of COSMOS/M were used to draw the wire frame of the bat. A series of curve commands were used to draw the outer shell of the bat. The bat is drawn to scale. The outside diameter of the barrel is 2.75 inches and the outside diameter of the handle is $0.855 \pm .006$ inches. The wall thickness varies from $0.0078 \pm .005$ inches to $0.110 \pm .004$ inches. However, for the model used in COSMOS/M, the wall thickness was assumed to be 0.1 inch throughout the entire length of the bat. This assumption was made because the bat was modeled as a thin shell with a shell thickness of 0.1 inches. For thin shells, COSMOS/M assumes that half of the shell thickness is added to one side of the wire frame and the other half of the thickness is added to the underside of the wire

frame. So, for a diameter of 2.75 inches with a radius of 1.375 inches, the radius of the curve drawn is 1.325 inches because the shell thickness of 0.1 inches adds 0.05 inches to the length of the radius making the final radius 1.375 inches. The length of the bat is 34.0 inches.

4.3 MESHING

Once the outline curves of the bat are drawn, these curves are then meshed. The automatic meshing feature of COSMOS/M was used to mesh the bat. When curves are meshed using this feature, two node elements are formed. For automatic meshing, the number of elements on the boundary or the average element size is chosen by the user.

4.3.2 Element Size

Before meshing, the number of elements on the boundary and the average element size of the elements must first be determined. The equation,

$$\hat{A} = r\theta$$

where \hat{A} is the arc length or length of the mesh, r is equal to the radius, and θ is equivalent to the angle, is used to compute the size of the mesh which determines the number of boundary elements.

For meshing purposes, the bat was broken into three sections: barrel, transition region, and handle. For the barrel, θ was equal to 18 degrees and r was equal to 1.375 inches. By using these numbers in the above equation, the mesh size, \hat{A} , is equal to

approximately 25 mesh elements. For the barrel end of the bat, 25 mesh elements will be around the circumference of the bat. For the transition region, θ was equal to 36 degrees and r was equal to 1.375 inches, therefore, the size of the mesh calculated was approximately 50 mesh elements. This same mesh size of 50 was also assumed for the bat's handle. Thus, for the transition region and the handle of the bat, there are 50 mesh elements around the bat's circumference.

4.3.3 Aspect Ratio

Once the mesh size is calculated, the element length, average size of the element, must then be determined. The aspect ratio is used to determine the element size. The aspect ratio can be found by using

$$\frac{B}{A} \leq 5$$

where B represents the long side of the element and A represents the element's short side. Before determining the size for the long side of the element, the short side must first be calculated by using

$$A = \frac{C}{\hat{A}}$$

where C is the circumference of the bat and \hat{A} is the mesh size. For the barrel, C is equal to 8.321 inches and \hat{A} is equal to 25; therefore, A is equal to 0.3328 inches.

The above inequality is met when B is assumed to be 0.5 inch. Therefore, the element length used for the barrel of the bat is 0.5 inch. For the handle, C is equal to 2.1949

inches and \hat{A} is equal to 50; therefore, A is equal to 0.0439 inches. The aspect ratio inequality is met when B is assumed to be 0.2 inches. Therefore, the element length used for the handle is 0.2 inches. This element length is also used for the transition region.

4.3.4 Automatic Meshing

Once the number of mesh elements and element length are determined, the bat is then meshed. Automatic meshing is used. When meshing curves by this method, two node elements are formed. These two node elements are then swept 360 degrees. The bat was meshed in sections: the barrel and the handle. The two node elements are now four node elements. A three dimensional meshed model of the bat has been formed.

4.3.5 Merging Nodes

Because the bat was meshed in two different sections, the two meshes must properly line up or be connected. In order to do this, the nodes must be merged. If the nodes are not properly merged, there will be bad element connectivity. The nodes were merged with a tolerance of 0.005 inches. By merging the nodes with a 0.005 inch tolerance, the two meshes are properly joined.

4.4 MATERIAL PROPERTIES

After the bat has been properly meshed, the bat's material properties must be defined. The material used for the bat model was an aluminum alloy. The following material properties were used for the aluminum alloy:

Modulus of elasticity = $1.0 \text{ e}+7 \text{ lbs} / \text{in}^2$

Poisson's ratio = $3.3 \text{ e}-1 \text{ in} / \text{in}$

Shear modulus = $3.9 \text{ e}+6 \text{ lbs} / \text{in}^2$

Coefficient of thermal expansion = $1.3 \text{ e}-5 \text{ in} / (\text{in}^\circ \text{F})$

Density = $2.5 \text{ e}-4 \text{ lbs sec}^2 / \text{in}^4$

Specific heat = $8.3 \text{ e}+1 \text{ BTU in} / \text{lbs sec}^2 / ^\circ \text{F}$

Thermal conductivity in the global X – direction = $2.7 \text{ e}-3 \text{ BTU} / \text{in sec}^\circ \text{F}$

All of these values are in the U.S. customary system of units.

Only one real constant was used and that is the shell thickness. This is assumed to be 0.1 inches.

4.5 END CAPS

Once the shell model of the bat was complete, the end caps had to be drawn. A single curve was drawn and then this curve was swept as a surface, thereby, making the end caps solid. The end caps were then meshed on the barrel and handle end of the bat.

4.5.2 Meshing the End Caps

The end caps were meshed by using the parametric meshing feature of COSMOS/M. For parametric meshing, the number of elements along the boundaries can be determined by the user.

The number of elements around the circumference of the bat was determined when the tube of the bat was meshed. This is the same number of elements that will be used around the circumference of the end caps. There are 25 elements for the barrel end cap, and 50 elements for the handle end cap.

The next step in the parametric meshing process was to determine how many elements would be along the radius of the end cap. The number of elements along the radius are first assumed and then the assumption is checked by the aspect ratio inequality,

$$\frac{B}{A} \leq 10,$$

B represents the length of the meshed elements along the boundary. This was calculated previously when meshing the tube of the bat. For the barrel end, $B = 0.33284$ inches, and for the handle, $B = 0.0439$ inches. A represents the average element size. The value of A is calculated by using

$$A = \frac{r}{l}$$

where r represents the radius for the end cap and l represents the number of meshed elements on the radius. For the barrel, $r = 1.325$ inches. By assuming $l = 5$, then $A = 0.265$ inches. When $A = 0.265$ inches, $\frac{B}{A} = 1.256$ and this satisfies the aspect ratio

inequality. Therefore, there should be 5 meshed elements on the radius boundary of the barrel end cap. For the handle, $r = 0.3495$ inches. By assuming $l = 10$, then $A = 0.03495$ inches. With this value for A , then $\frac{B}{A} = 1.256$ and this satisfies the aspect ratio inequality. Thus, there should be 10 meshed elements on the radius boundary.

After the number of elements on the circumference and the radius boundaries are determined, the end caps can be meshed. Parametric meshing was used to mesh the surface of the end caps. Triangular shaped elements were used in the meshing process. For the barrel end cap, there are 25 elements around the outer edge of the end cap and 5 elements along the radius of the end cap. For the handle end cap, there are 50 elements along the outer edge and 5 elements along the radius of the end cap.

After the meshing was complete, the nodes had to be merged. Merging the nodes connects the node of the end cap meshes to the nodes of the meshed tube of the bat. A tolerance equal to 0.005 inches was used.

The complete drawing of the bat can be seen in Figure 20.

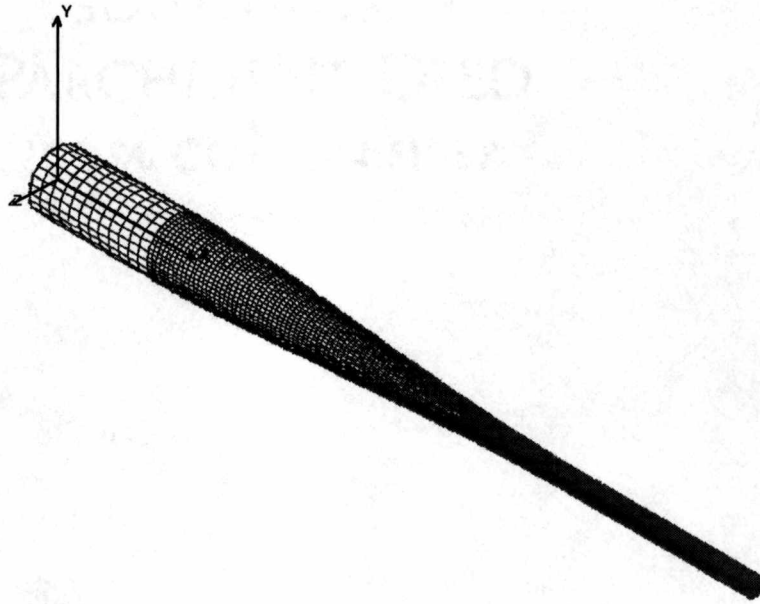


Figure 20: Model drawing of the bat used in the COSMOS analysis.

4.6 DISPLACEMENTS

After the model of the bat has been completely meshed, it is now important to apply the displacements to the bat. The bat has six degrees of freedom. For this project, the six degrees of freedom at the bat's handle were set to zero. In other words, there can be no displacement at the bat's handle. It is as though the bat were clamped in a vise at the handle.

4.7 LOADS

After the boundary conditions or displacements have been set, the next step is to apply the appropriate loads. An assumed load of 100 pounds is applied at node 306 in the negative z direction. Node 306 was picked because it is approximately in the center of the barrel section of the bat. The 100-pound load was used for the static analysis. After the static analysis was completed, the load was changed to 1 pound. The reason for changing the force to 1 pound was because in the time history analysis, the actual mass of 100 pounds was applied to the bat. This mass is multiplied by the mass of the force that is applied directly to the bat. The force that is applied to the bat represents the force of the ball impacting the bat.

4.8 GEOMETRICAL CHANGES

The next step in modeling the bat was to add a geometrical change. A geometrical change was added at various places in the bat: 31.54, 40.36, 49.19, and 58.01 percentages from the barrel end of the bat.

4.8.2 Creating the Geometrical Change

The geometrical change was created by first using four curves to draw a rectangle with the two long sides equal to the bat's radius. The width of the geometrical change was the same as the length of the element located at the geometrical change's position. These four curves were then changed into a surface. The surface was then swept as a volume broken into five sections. This created a solid geometrical change.

4.8.3 Meshing the Geometrical Change

After the geometrical change was drawn, it then had to be meshed. Once again, parametric meshing was used. The mesh of the geometrical change has to coincide with the mesh of the bat tube. In other words, the elements have to line up together. For this parametric meshing technique, quadrilateral or eight node solid elements were used instead of the triangular elements used to mesh the end caps. Since the geometrical change was meshed as a solid, not only does the user have to choose the number of elements around the circumference and along the radius of the geometrical change, but the number of elements across the width of the geometrical change must also be chosen.

Because the mesh of the geometrical change and the mesh of the bat have to coincide, the number of elements around the circumference of the geometrical change and the bat must equal. At every geometrical change location, there are 50 elements around the circumference.

For the barrel end cap, there were 5 elements along the radius boundary. Since the barrel end cap and the geometrical change centered at 31.54% and the one to be centered at 40.36% are similar in size, there will also be 5 elements along the radius boundary of the geometrical change. For the geometrical change at 49.19% there were 4 elements located along the boundary of the radius and 3 at 58.01%.

Next, the number of elements along the width of the geometrical change must be determined. This number was arbitrarily chosen as 1 for all geometrical changes. The reason for this choice was because the width of the geometrical change was equal to the length of one element in the bat's mesh. These numbers were checked against the aspect

ratio inequality that was used previously. The inequality was met for an aspect ratio less than or equal to 10.

4.8.4 Connection of Geometrical Change to the Bat

After the geometrical change has been meshed, the nodes must be merged. This is what will connect the mesh of the geometrical change to the mesh of the bat. A tolerance of 0.005 inches was used.

4.8.5 Element Groups

Another element group also has to be formed for the geometrical change. The bat itself is modeled as a thin shell. The geometrical change has to be modeled as a solid; however, the material properties remain the same. Both the geometrical change and the bat are made from aluminum alloys.

4.9 ANALYSIS

COSMOS was used to analyze the bats. A linear static, frequency, and a post dynamic analysis were all performed on the bats.

4.9.2 Static Analysis

Once the bat was modeled with and without the geometrical changes, a static analysis was performed on the bat without any geometrical changes and then on the bat with the geometrical changes in place. The static analysis was used in order to check the

stiffness of the bat. Checking the stiffness is a way to check and see if adding a geometrical change added mass or stiffness. The results of this analysis can be seen in Chapter 5.

4.9.3 Frequency Analysis

After a static analysis was completed, a frequency analysis was performed on all the bats: the baseline model bat, the bat with no geometrical change, and the four bats with the geometrical changes in place. A separate analysis was made for each new location of the geometrical change. For example, there was a complete natural frequency analysis for the bat with a geometrical change centered at 31.54% and then there is a complete natural frequency analysis for a bat with a geometrical change centered at 40.36% , 49.19%, and 58.01%. Twenty modes were calculated for each bat.

4.9.4 Post-Dynamic Analysis

After the frequency analysis was completed, a post-dynamic analysis was also performed on the bat. The results from the previous frequency analysis were used in this analysis. A time history analysis was used for the post-dynamic analysis. In this type of analysis, the number of time step and the iteration size for the time step must be chosen. For this particular analysis, the time step chosen was 0.001 seconds and there were 200 time steps. Therefore, the time history had duration of 0.2 seconds. A load of 100 pounds was applied at .005 seconds. At a time equal to 0.0085 seconds, the load was completely removed. The force was in contact with the bat for .0035 seconds because

this is approximately the length of time a ball is in contact with the bat. For the results, the nodes that were being studied were chosen before the analysis was performed. Nodes were chosen at the tip of the barrel, the point of contact with the force, the transition region and the tip of the handle. The Newmark-Beta integration method was chosen and then the post-dynamic time history analysis was started. These results can be seen and explained in Chapter 5.

5. RESULTS

5.1 LINEAR STATIC ANALYSIS

A linear static analysis was the first type of analysis performed on the baseline model bat, the bat without any form of geometrical change. It can also be used to check displacement and the stiffness of the bat. This same analysis was performed on one of the bat's that contained a geometrical change. A comparison was made between the static results of the baseline model bat and the bat with the geometrical change. These results are shown in Table 1.

Table 1: Bat Displacements.

<i>Node</i>	<i>Displacements in Z Dir. (in.)</i>	
	<i>Base Model</i>	<i>Geometrical change at 31.54%</i>
1	-5.084e+00	-5.084e+00
75	-2.103e+00	-2.103e+00
175	0.0	0.0
306	-4.646e+00	-4.646e+00

Node 1 is located at the barrel end of the bat. Node 75 is located in the bat's transition region and the tip of the handle is represented by node 175. The ball impacts the bat at node 306. The location of these nodes on the bat can be seen in Figure 21.

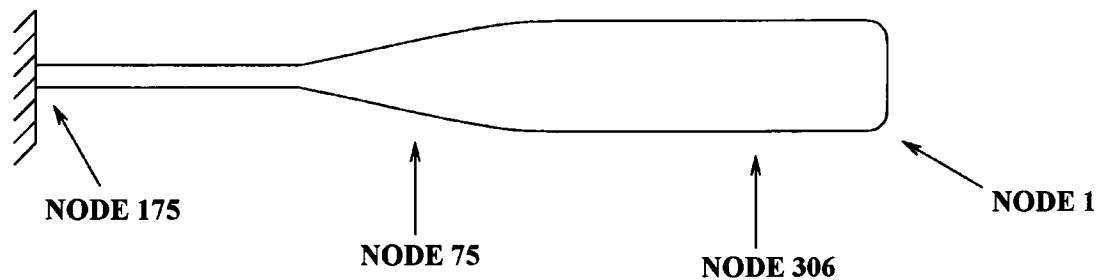


Figure 21: The locations of the referenced nodes on the bat.

When a geometrical change is added to the bat, there is an increase in the bat's mass. From the results in Table 1, it can be seen that the displacements of the two bats are the same. This shows that a bat's stiffness is not changed when a geometrical change is added to the bat.

Since this analysis was just used as a method for checking to see if the addition of a geometrical change added stiffness to the bat, it was only performed on one of the bats with a geometrical change. There was no need to repeat the analysis for the other bats because if the addition of the geometrical change added only mass and not stiffness in one bat, the other bats would experience the same effect.

5.2 FREQUENCY ANALYSIS

After it was determined that the addition of the geometrical change only added mass and not stiffness, a frequency analysis was performed on the baseline model and four different bats with geometrical changes centered at different locations. The locations for the geometrical changes are 31.54%, 40.36%, 49.19% and 58.01%. All percentages are measured from the barrel end of the bat. For all five bats, twenty modes of the natural frequencies were calculated. The subspace iteration method was used to calculate these frequencies. It was decided to use only the first twenty natural frequencies because these frequencies sufficiently satisfy the elastic behavior of a bat after it has been struck by a ball (Van Zandt, 1991, p.175). These twenty natural frequencies for all the bats can be seen in Table 2.

These results were then studied and comparisons were made. From the results, it can be seen that the various locations of the geometrical change affect the bat's various frequencies differently. For a geometrical change centered at 31.54%, the first ten frequencies are lower than for the baseline model bat. The first two frequencies are of special interest in this study. Of all four bats studied, the first two frequencies are the lowest for the bat with a geometrical change centered at 31.54% from the barrel end. A change in the first two frequencies also changes the response of the bat after impact with the ball. This is the intended effect for the optimum location of the geometrical change in a bat.

Table 2: Natural frequencies for baseline model bat and for bats with a geometrical change centered at 31.54%, 40.36%, 49.19%, and 58.01% from the barrel end.

<i>Frequency Number</i>	<i>Frequency Percent Change</i>			
	<i>Modification @ 31.54%</i>	<i>Modification @ 40.36%</i>	<i>Modification @ 49.19%</i>	<i>Modification @ 58.01%</i>
1	1.89	0.85	0.30	0.05
2	1.89	0.84	0.30	0.05
3	1.18	1.11	0.97	0.61
4	0.99	1.84	1.92	1.35
5	1.14	1.29	1.12	0.73
6	1.43	1.01	0.05	0.08
7	1.39	0.99	0.02	0.07
8	2.47	1.44	0.64	0.21
9	1.14	0.05	0.78	1.51
10	1.15	0.05	0.84	1.51
11	5.97	0.28	0.01	0.00
12	5.98	0.28	0.01	0.00
13	0.09	0.88	1.35	0.05
14	0.06	1.10	1.39	0.04
15	18.00	6.15	0.03	0.00
16	33.14	6.15	0.03	0.00
17	14.01	0.78	0.14	0.51
18	0.45	1.73	0.02	1.34
19	0.68	1.29	0.26	1.08
20	13.32	14.34	0.92	0.00

There is a unique deformed shape of the bat at each natural frequency. For modes 1, 2, and 3, the corresponding bat deformation can be seen in Figures 22 – 24 for the baseline model bat and in Figures 25 - 27 for the bat with a geometrical change centered at 31.54%.

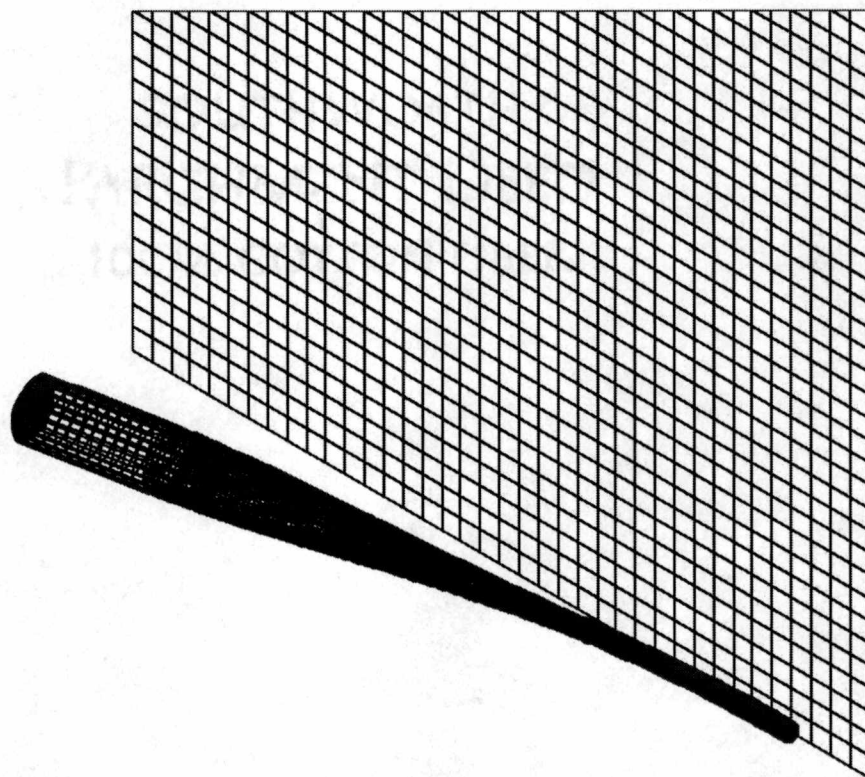


Figure 22: Mode 1 deformed shape for the baseline model bat.

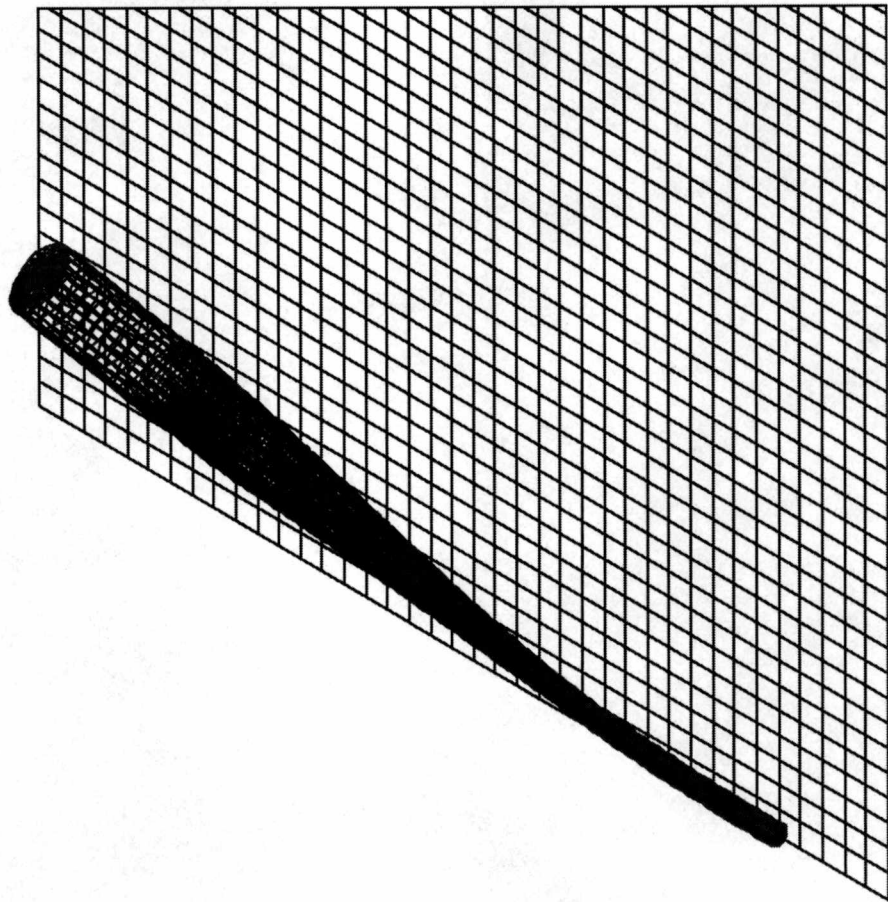


Figure 23: Mode 2 deformed shape for the baseline model bat.

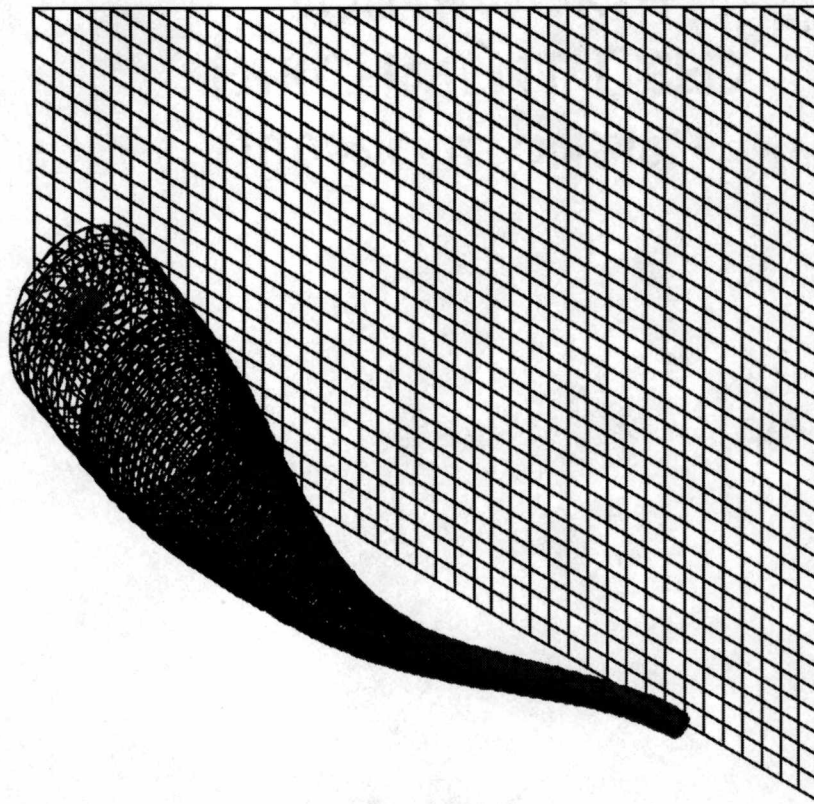


Figure 24: Mode 3 deformed shape for the baseline model bat.

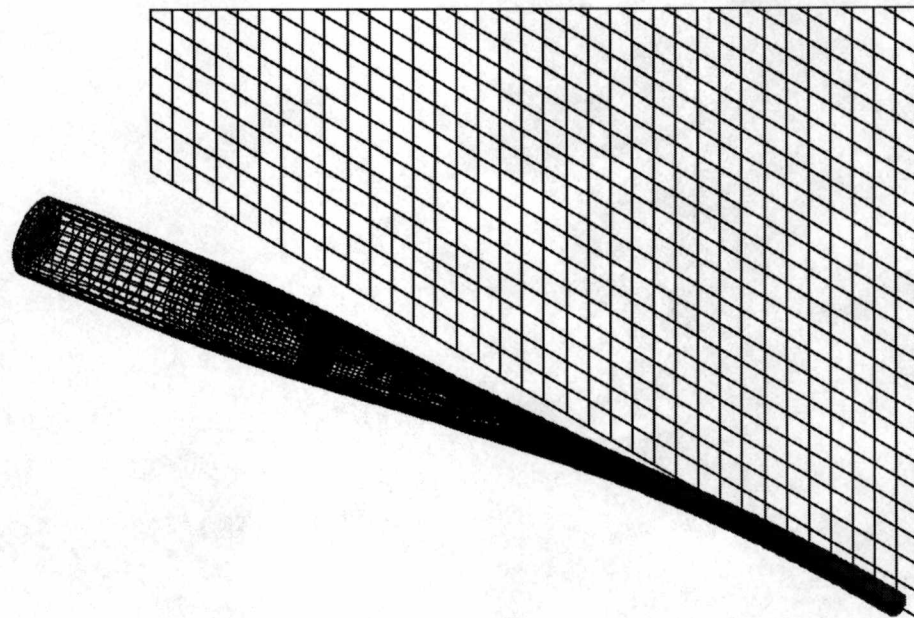


Figure 25: Mode 1 deformed shape for the bat with a geometrical change centered at 31.54%.

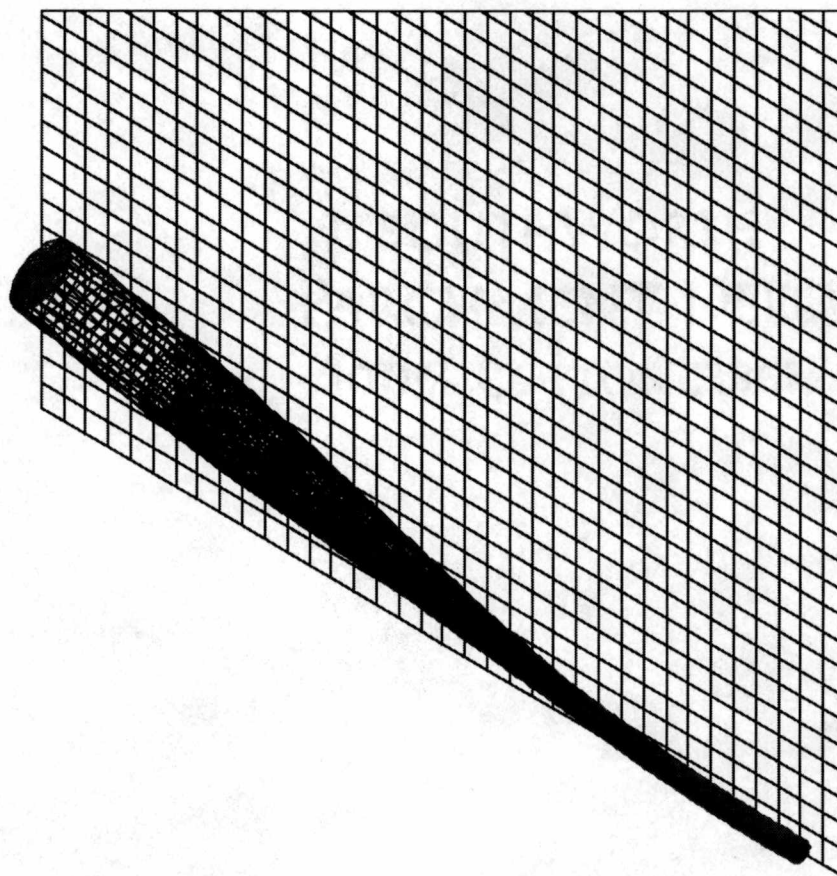


Figure 26: Mode 2 deformed shape for the bat with a geometrical change centered at 31.54%.

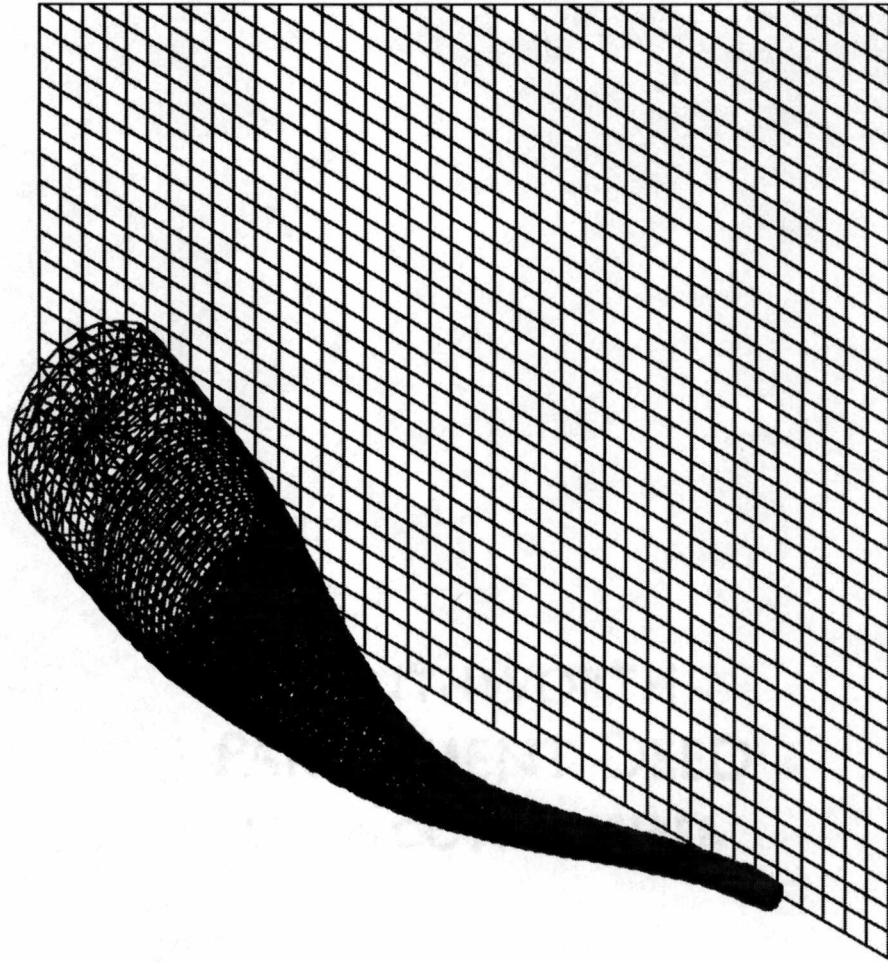


Figure 27: Mode 3 deformed shape for the bat with a geometrical change centered at 31.54%.

For both bats, the first and second modes are graphical representations of simple bends. Since the bat is clamped, these first two frequencies are lower in value than if the bat were free. When the bat is held clamped at the handle, there is a longer moment arm about which the bat has to swing (Van Zandt 1991). From Figures 22 - 27, it can also be seen that as the mode number increases so does the number of nodes in the shape of the bat. For example, for modes 1 and 2, there was 1 node. For mode 3 of both bats, there were 2 nodes. This progression continues for all proceeding frequencies. Also, for the

lower frequencies, the oscillations are in the bat's handle. For the higher modes of vibration for the natural frequencies, the oscillations start occurring in the barrel portion of the bat.

5.2.2 Acrylic Versus Aluminum

The geometrical changes used in the bats were made from aluminum (almost the same material as the bats). However, the composition of one of the geometrical changes was made from an acrylic. The material properties of acrylic are as follows:

Modulus of elasticity = $3.5 \text{ e}+5 \text{ lbs} / \text{in}^2$

Poisson's ratio = $3.5 \text{ e}-1 \text{ in} / \text{in}$

Shear modulus = $1.3 \text{ e}+5 \text{ lbs} / \text{in}^2$

Coefficient of thermal expansion = $2.9 \text{ e}-5 \text{ in} / (\text{in}^\circ F)$

Density = $1.1 \text{ e}-4 \text{ lbs sec}^2 / \text{in}^4$

Specific heat = $1.4 \text{ e}+2 \text{ BTU in} / \text{lbs sec}^2 / ^\circ F$

Thermal conductivity in the global X – direction = $2.8 \text{ e}-6 \text{ BTU} / \text{in sec}^\circ F$.

This geometrical change was placed in a bat at 49.19% from the barrel end. A frequency analysis was performed on this bat. These results were compared to a bat with a geometrical change with a composition of aluminum centered at 49.19% from the barrel end. The results from this analysis can be seen in Table 3.

Table 3: Aluminum geometrical change frequency versus acrylic geometrical change frequency.

<i>Frequency Number</i>	<i>Frequency Percent Change</i>	
	<i>Aluminum Geometrical Change</i>	<i>Acrylic Geometrical Change</i>
1	0.30	0.69
2	0.30	0.68
3	0.97	2.53
4	1.92	4.40
5	1.12	2.19
6	0.05	0.42
7	0.02	0.36
8	0.64	1.61
9	0.78	1.74
10	0.84	1.88
11	0.01	0.01
12	0.01	0.01
13	1.35	3.03
14	1.39	3.11
15	0.03	0.03
16	0.03	0.03
17	0.14	0.41
18	0.02	0.07
19	0.26	0.57
20	0.92	0.92

From Table 3, it can be seen that the frequency for the acrylic geometrical change is lower for the first 19 modes of frequency. For mode 20, the frequency of the acrylic geometrical change was higher. These differences in frequencies between the aluminum and acrylic geometrical changes are only marginal. Although the differences in the frequencies are marginal, the results of this analysis show that the geometry of the geometrical change along with its material composition can reflect changes in the bat's frequency. This is a desired result.

5.2.3 Wall Thickness

For the bat, a wall thickness equal to 0.1 inches was assumed. However, for a comparison, another bat was calculated with an assumed wall thickness of 0.05 inches. A geometrical change was also placed at 31.54% from the barrel end. A frequency analysis was performed on this bat and compared to the original bat with a wall thickness of 0.1 inches. The results and comparison can be seen in Table 4.

Table 4: Percentage variations in frequency from baseline model bat for bats with different wall thickness.

<i>Frequency Number</i>	<i>Frequency Percent Change</i>	
	<i>0.1 In. Wall</i>	<i>0.05 In. Wall</i>
1	1.89	0.49
2	1.89	2.17
3	1.18	23.10
4	0.99	2.29
5	1.14	0.85
6	1.43	6.10
7	1.39	1.42
8	2.47	4.25
9	1.14	17.70
10	1.15	18.70
11	5.97	16.70
12	5.98	16.60
13	0.09	9.84
14	0.06	9.13
15	18.00	14.10
16	33.14	9.55
17	14.01	22.20
18	0.45	31.50
19	0.68	33.40
20	13.32	25.30

The results from this analysis show that the wall thickness does have a pronounced effect on the natural frequency of the bat. The bat's first natural frequency is increased and the second, third, and fourth natural frequencies are decreasing. There is one drawback to the frequency changing with wall thickness, below a minimum wall thickness, the bat will be damaged.

5.2.4 New Mesh

Due to some questions about the mesh distribution of the bat, a new uniform density mesh was applied to the bat. This new mesh is shown in Figure 28.

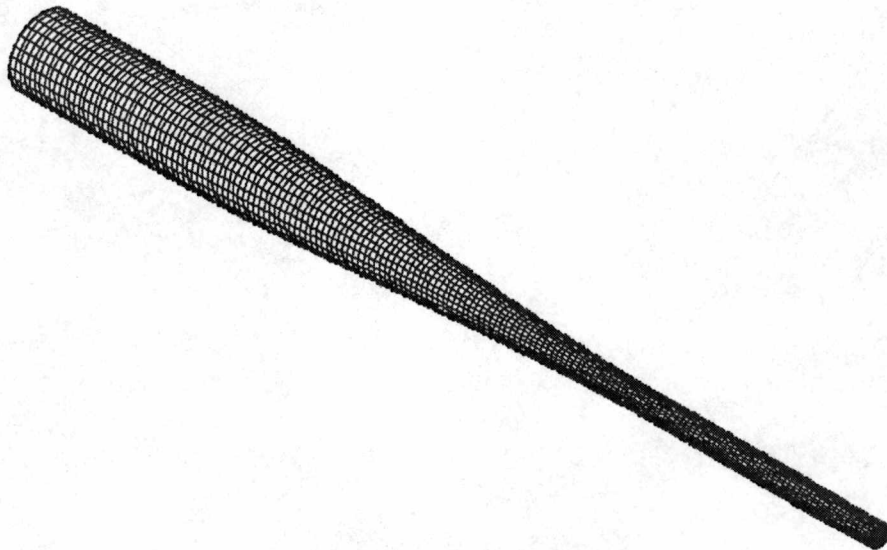


Figure 28: Bat with the new mesh.

A frequency analysis was then performed on the newly meshed baseline model bat and on the bat with a geometrical change centered at 31.54% from the barrel end of the bat. The results for the percentage difference between the baseline frequency and the frequency for the bat with a geometrical change are presented in Table 5.

Table 5: Percentage variations in frequency from baseline model bat for bat with a geometrical change centered at 31.54% from the barrel end of the bat.

<i>Frequency Number</i>	<i>Frequency Percent Change</i>
1	1.66435
2	1.67257
3	0.39936
4	1.05458
5	0.63256
6	0.0328
7	0.01388
8	0.3827
9	0.35121
10	0.38044
11	5.85995
12	5.88205
13	1.27898
14	1.44639
15	16.6707
16	32.3038
17	15.3867
18	1.87537
19	0.58061
20	11.9129

The overall analysis results in terms of frequency as well as displacement were very similar for the two mesh distributions. The results of the frequency analysis show that adding a geometrical change does affect the frequency of the bat. This was the desired effect. This is also compliant with the frequency analysis results that were performed on the bats with the previous mesh.

5.3 POST DYNAMIC ANALYSIS

After the frequency analysis was completed, a post-dynamic analysis was performed on the baseline model bat, the bat with the geometrical change centered at 31.54% and the bat with the geometrical change centered at 40.36%. The post-dynamic analysis was not performed on either the bat with a geometrical change centered at 49.19% or the bat with a geometrical change centered at 58.01%. It was decided that geometrical changes at these two locations were not as beneficial as the changes centered at 31.54% or 40.36%. This decision was based on the frequency analysis of each bat.

The twenty modes of the natural frequency were used in the post-dynamic analysis. There were 200 iterations with 0.001 seconds as the time step; therefore the analysis lasts for 0.2 seconds. A load of 100 pounds was applied at 0.005 seconds and the load stayed in contact with the bat for 0.0035 seconds. The relative displacement was calculated for this impact loading condition for 200 iterations using the Newmark-beta integration process. Figure 29 (Noble and Walker 1994) shows a characteristic vibration waveform for a bat stuck near the barrel end.

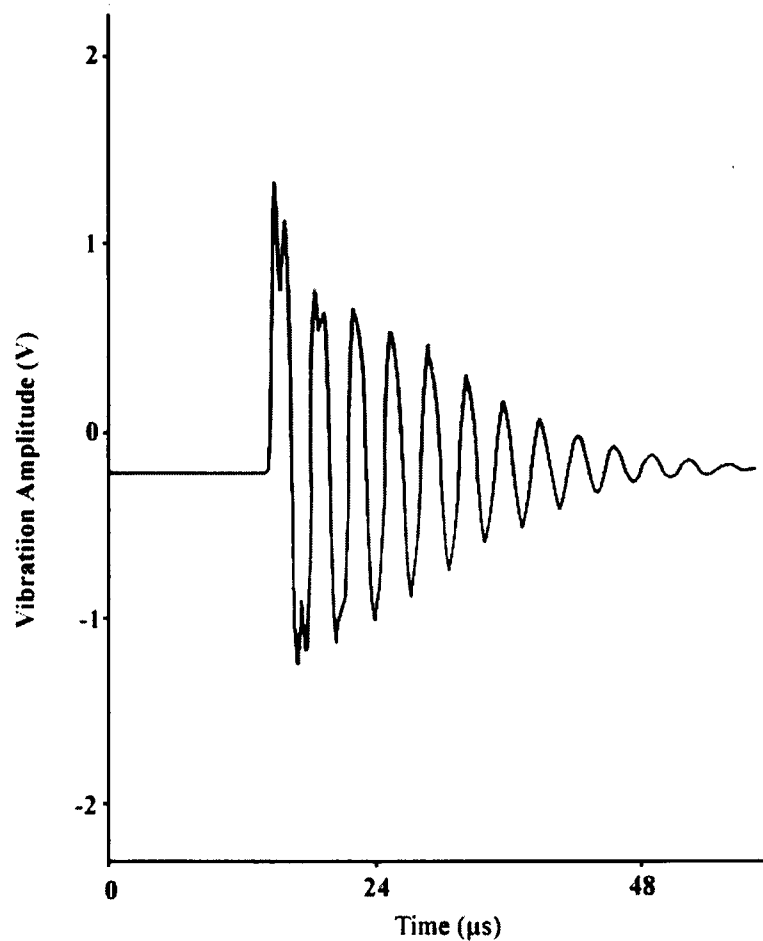


Figure 29: Vibrational amplitude versus time for a bat struck in the barrel region (Noble and Walker, 1993).

From this plot it can be seen that the vibration damps out around 48.0 microseconds. Vibrational waveform plots similar to those in Figure 29 were used to study the damping affects of the geometrical changes in this analysis.

5.3.2 Displacement Versus Time Curves

A plot of the relative displacement versus time for the baseline model bat can be seen in Figure 30. Figures 31 and 32 are plots of the relative displacement versus time

for the bat with a geometrical change centered at 31.54% from the barrel end and for the bat with a geometrical change centered at 40.36% from the barrel end, respectively. For each bat, the plots were made at mesh nodes 1 (tip of barrel), 75 (transition region), 175 (the tip of the handle), and 306 (place of impact).

Figure 30: Displacement versus time curves for the baseline model bat. The bat was impacted at node 306 with a force of 100 pounds. Displacement curves were plotted for nodes 1 (tip of the barrel), 75 (transition region), 175 (handle end), and 306 (point of impact and approximately middle of the barrel). The impact lasted for 0.0035 seconds.

Displacement Versus Time for Baseline Model Bat

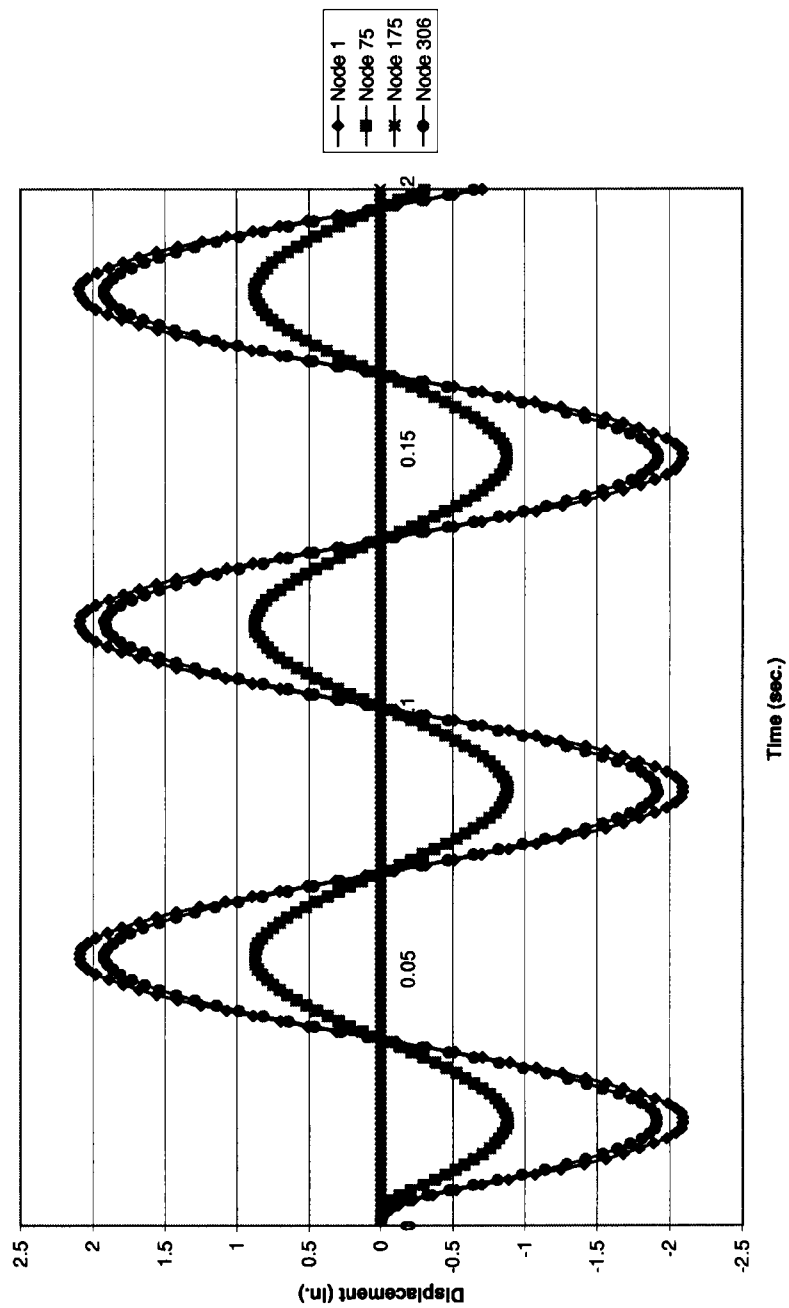


Figure 31: Displacement versus time curves for the bat with a geometrical change centered at 31.54% from the barrel end of the bat. The bat was impacted with a 100-pound force at node 306. Displacement curves were plotted for nodes 1 (tip of the barrel), 75 (transition region), 175 (handle end), and 306 (point of impact and approximately middle of the barrel). The impact lasted for 0.0035 seconds.

Displacement Versus Time for Bat with a Geometrical Change Centered at 31.54%

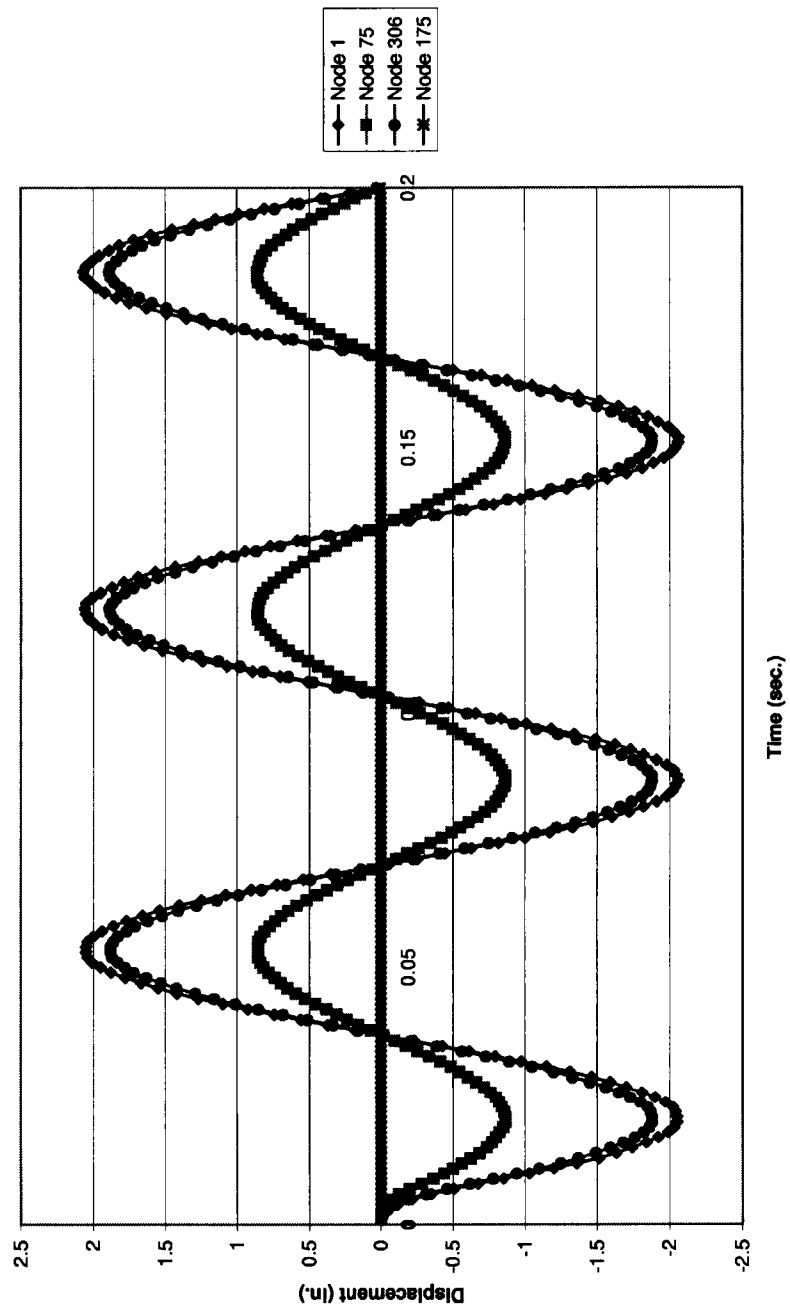
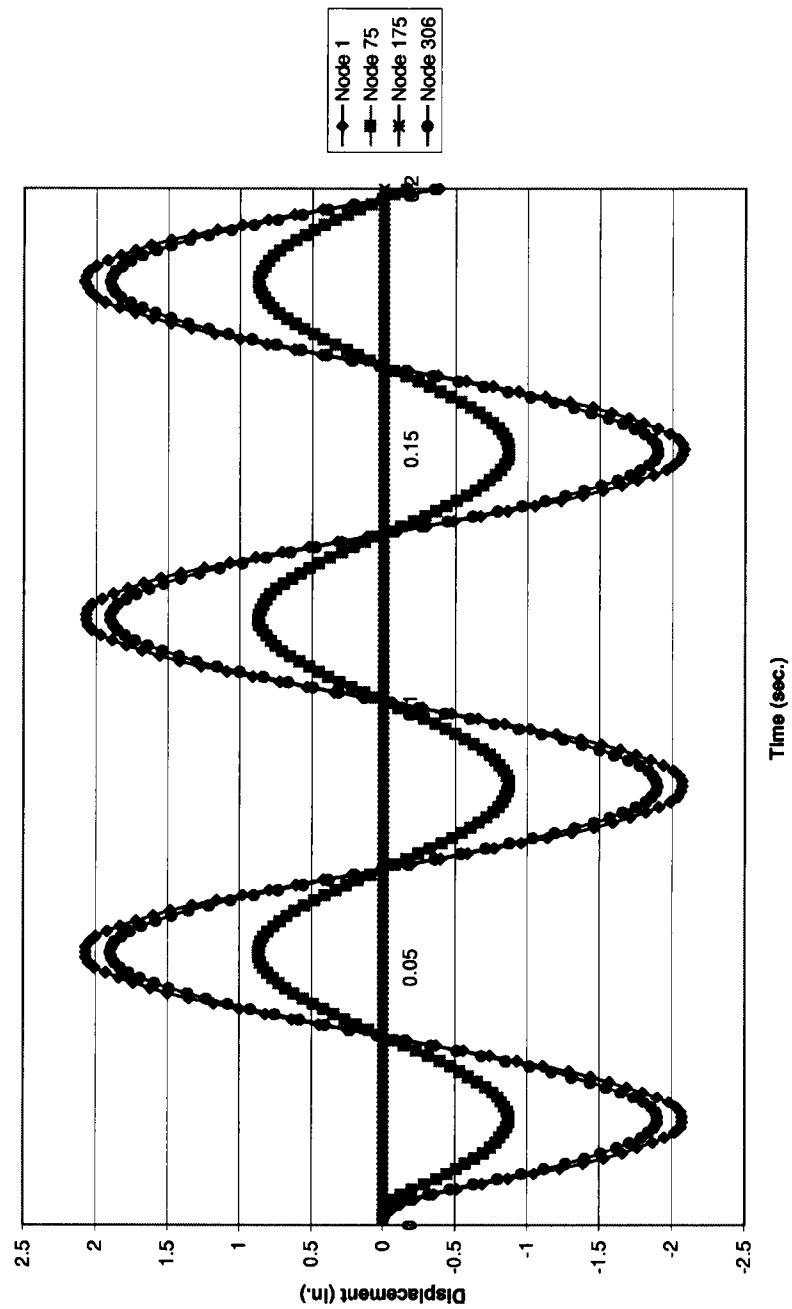


Figure 32: Displacement versus time curves for the bat with a geometrical change centered at 40.36% from the barrel end of the bat. The bat was impacted with a 100-pound force at node 306. Displacement curves were plotted for nodes 1 (tip of the barrel), 75 (transition region), 175 (handle end), and 306 (point of impact and approximately middle of the barrel). The impact lasted for 0.0035 seconds.

Displacement Versus Time for Bat with a Geometrical Change Centered at 40.36%



These plots show the amplitudes and frequency of vibration for the bat after a 100-pound force lasting 0.0035 second has impacted it. The period is the time it takes an oscillation to repeat itself. The frequency is the reciprocal of the period of an oscillation.

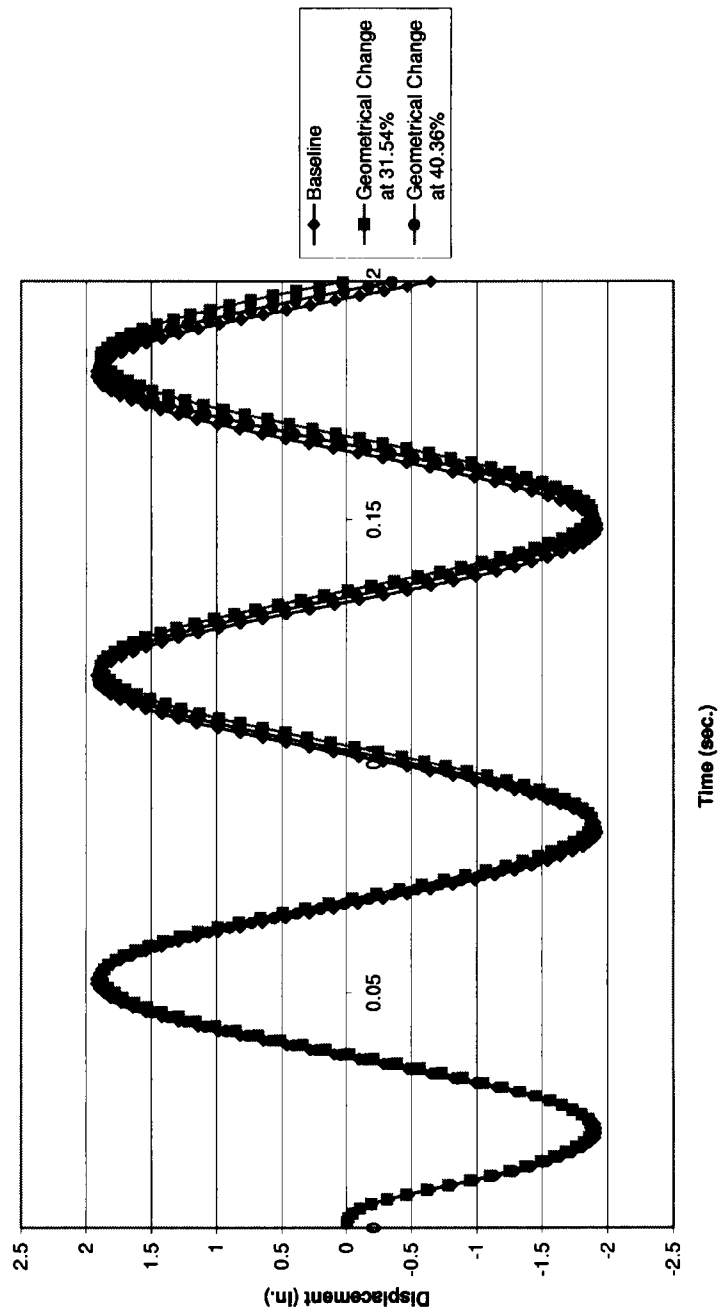
For all three bats, the displacement was the greatest at node 1, which was the tip of the barrel. The next greatest area of displacement was at node 306, point of impact. Node 175 had no degrees of freedom; therefore, there was no displacement at this point.

From these figures, it can be seen that as time increased the amplitude of the oscillations gradually begins to decrease. The frequency of the oscillations also begins to decrease as time increased. This occurred in all three bats.

Although the plots for the three bats look similar, if the three plots are combined as in Figure 33, it can be seen that there is a difference can be seen in the graphs. Figure 33 is a displacement versus time curve at node 306 for the baseline model bat, the bat with a geometrical change centered at 31.54% from the barrel end of the bat, and the bat with a geometrical change centered at 40.36% from its barrel end.

Figure 33: Combined displacement versus time curves. The displacement curves are for the baseline model bat, the bat with a geometrical change centered at 31.54% from the barrel end, and the bat with a geometrical change centered at 40.36% from the barrel end of the bat. All three plots represent node 306, which was the point of a 100-pound impact force.

Combined Displacement Versus Time Curves at Node 306 for the Baseline Model Bat, the Bat With a Geometrical Change Centered at 31.54%, and the Bat With a Geometrical Change Centered at 40.36%



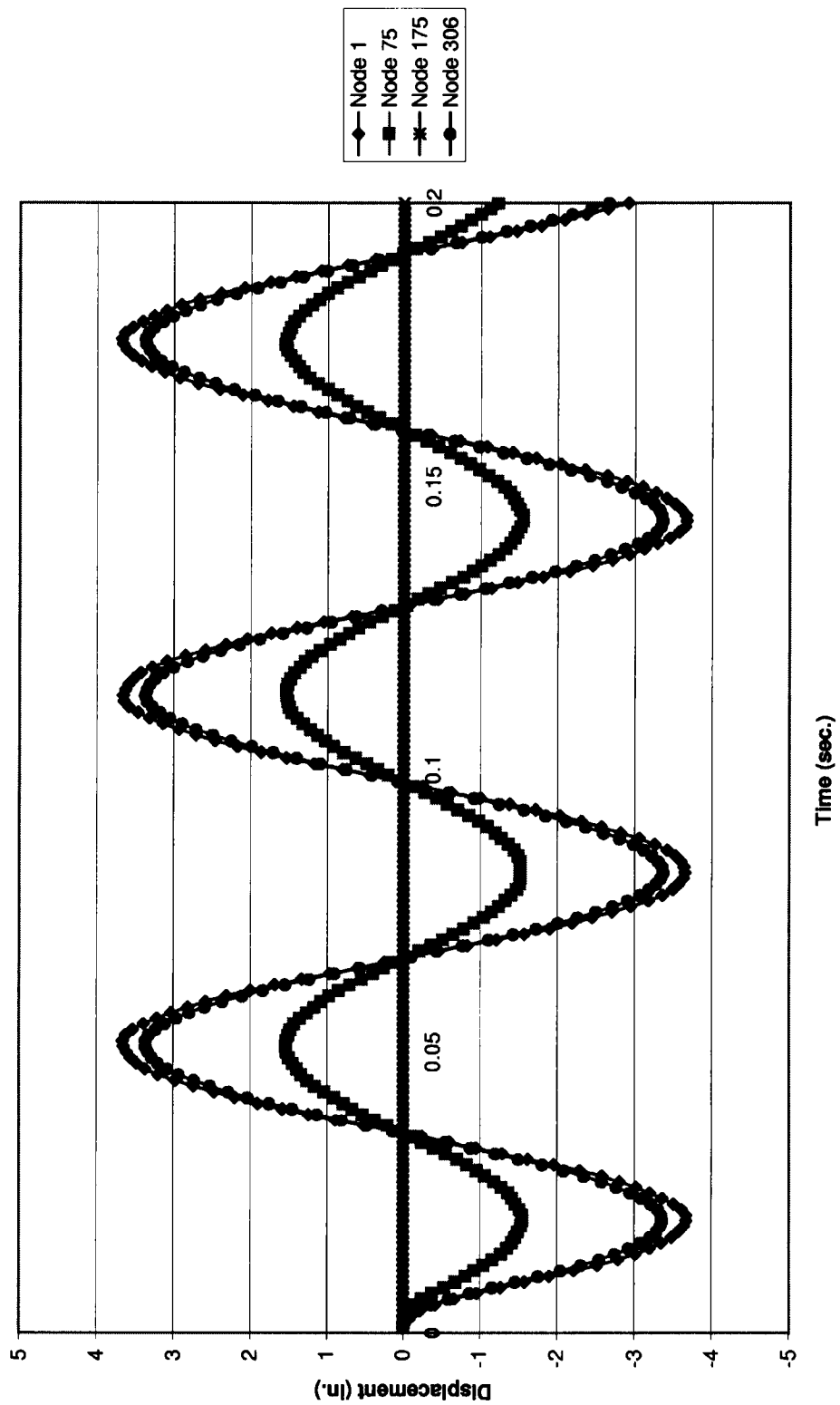
The frequency for the bat with the geometrical change centered at 31.54% has shifted more to the right than the frequency of the other two bats. The bat with the geometrical change centered at 40.36% has a frequency that has shifted more than that of the baseline model bat. Because the displacement versus time plots at the same node for the three bats are different, it shows that the containment and placement of a geometrical change in a bat greatly affects the bat's vibration. The plots have shown that the bats containing geometrical changes have amplitudes of vibration that begin to damp out quicker than the bat that does not contain a geometrical change, the baseline model bat. It has also been shown that the frequency of oscillations of the bat with a geometrical change centered at 31.54% shift more to the right than the bat with the geometrical change centered at 40.36%. This shows that the placement or location of the geometrical change in the bat is also of great importance to reducing the vibrations in a bat. Therefore, an optimum location of a geometrical change in a bat would greatly optimize a bat by aiding in the reduction of vibration.

5.3.3 Shell Thickness Affect

Once it was decided that the geometrical change at 31.54% was the optimum place for the geometrical change, the other bats with geometrical changes were no longer studied. The next bat that was analyzed using the model time history was a bat with a shell thickness of .05 inches. A plot for relative displacement versus time for this bat can be seen in Figure 34.

Figure 34: Displacement versus time curves for the bat with a wall thickness of 0.05 inch and containing a geometrical change centered at 31.54% from the barrel end of the bat. The bat was impacted at node 306 with a 100-pound force. Displacement curves were plotted for nodes 1 (tip of the barrel), 75 (transition region), 175 (handle end), and 306 (point of impact and approximately middle of the barrel). The impact lasted for 0.035 seconds.

Displacement Versus Time for Bat with 0.05 Inch Wall Thickness

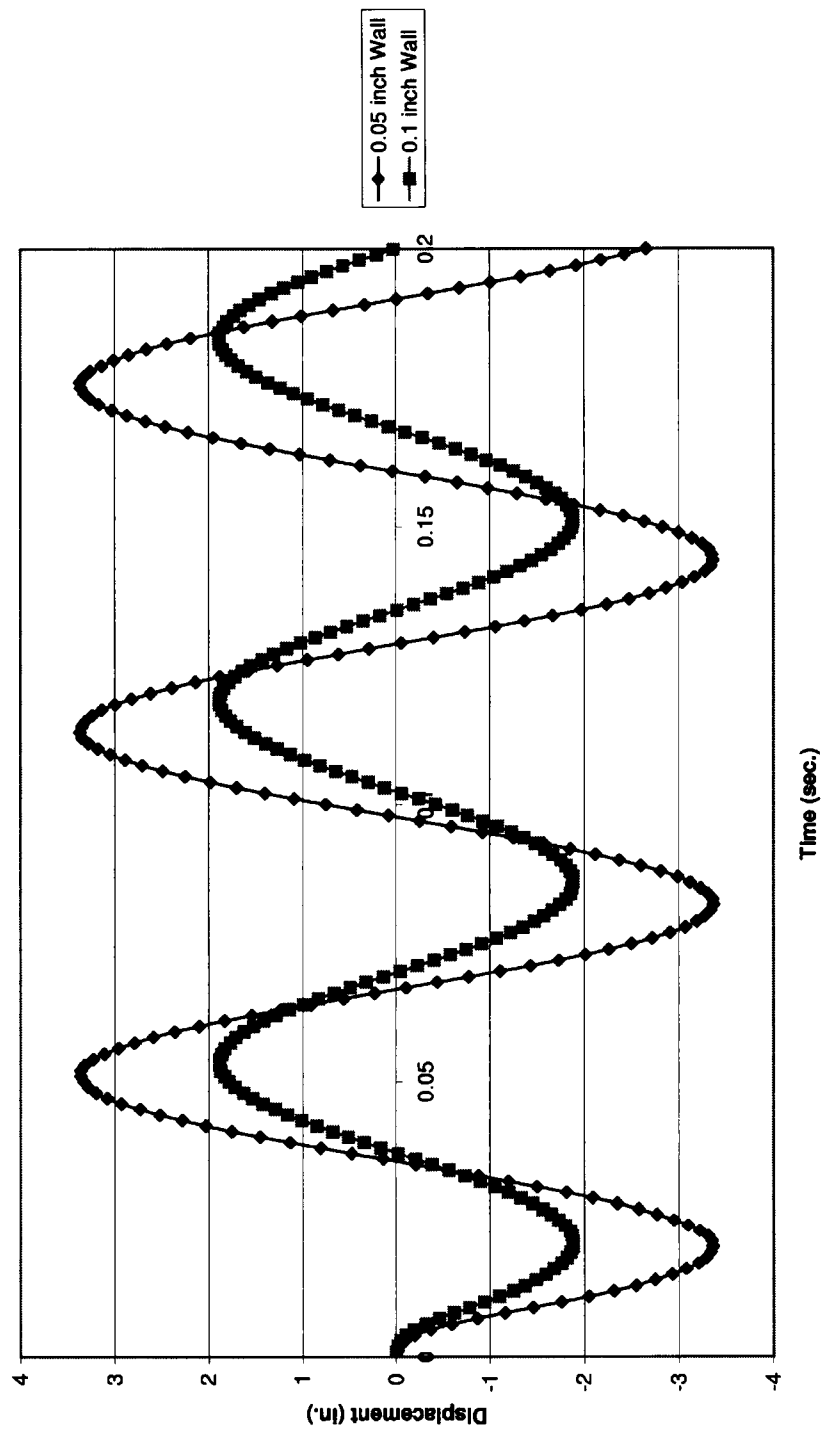


When the wall thickness was reduced, the bat became more flexible and easier to bend. It is readily seen, when comparing Figure 31 to Figure 34 that the 0.05-inch thick walled bat's displacement is larger in amplitude than that of the bat with a wall thickness of 0.1 inches. The displacement is larger in the thinner shelled bat because it will bend easier.

Figure 35 is a plot of the displacement versus time at node 306 for a bat with a wall thickness of 0.05 inch and a bat with a wall thickness of 0.1 inch. Besides having lower displacement amplitude, the thicker shelled bat's period shifts more to the right than the thinner shelled bat.

Figure 35: Displacement versus time curves for the bat with a wall thickness of 0.05 inch and for the bat with a wall thickness of 0.1 inch. Both bats contain a geometrical change at 31.54% from the barrel end of the bat. The displacement curves are for node 306, the point of impact on the bat.

Displacement Versus Time at Node 306 for Bat with wall Thickness of 0.05 Inches and for Bat
with Wall Thickness of 0.1 Inches



5.4 EXPERIMENT

An experiment that measured sound amplitude was also performed on the base model bat and the bat with a geometrical change centered at 31.54% from the barrel end. The bat's sound amplitude was measured because the vibration of a bat is directly proportional to the sound amplitude.

For the experiment, the handle of a bat was clamped. A microphone was placed near the middle section of the barrel and one was placed at the tip of the barrel. The bat was then impacted in the middle of the barrel region. The microphones were then used to measure the sound amplitude of the bat. Figure 36 is a drawing of the experiment setup.

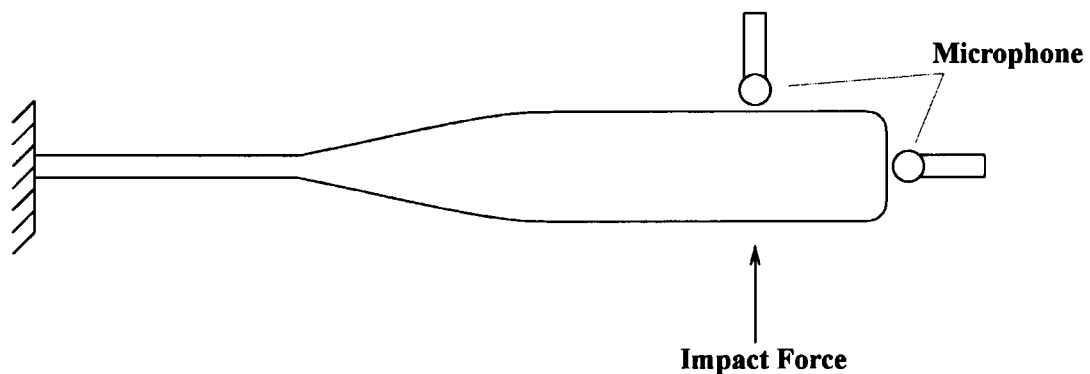


Figure 36: Experiment setup for measuring the sound amplitude of a bat after impact.

Energy versus frequency plots of the Fourier transforms of the microphone signals can be seen in Figures 37-38. Figure 37 is the Fourier transform of the microphone signal of the base model bat and Figure 38 represents the bat with a geometrical change centered at 31.54%.

According to the Fourier transform of the microphone signals, the bat with a geometrical change centered at 31.54% has a single specific frequency of vibration. It can be seen in Figure 37 that the base model bat does not have a single frequency of vibration but many frequencies. When the energy is spread out over many frequencies, a lot of energy is being lost. However, when there is a single specific frequency peak, most of the energy is concentrated at and around this specific frequency peak. More energy is present at the specific frequency than the energy that is distributed through the many frequencies. If energy is integrated for the many frequencies of the base model bat and for the specific frequency of the bat with the geometrical change centered at 31.54%, the sum of the distributed integrated energy from the base model bat will be similar to the integrated energy at the specific frequency of the bat containing the geometrical change.

Figure 37: Fourier transform of the sound amplitude for the baseline model bat. The energy is distributed over many frequencies.

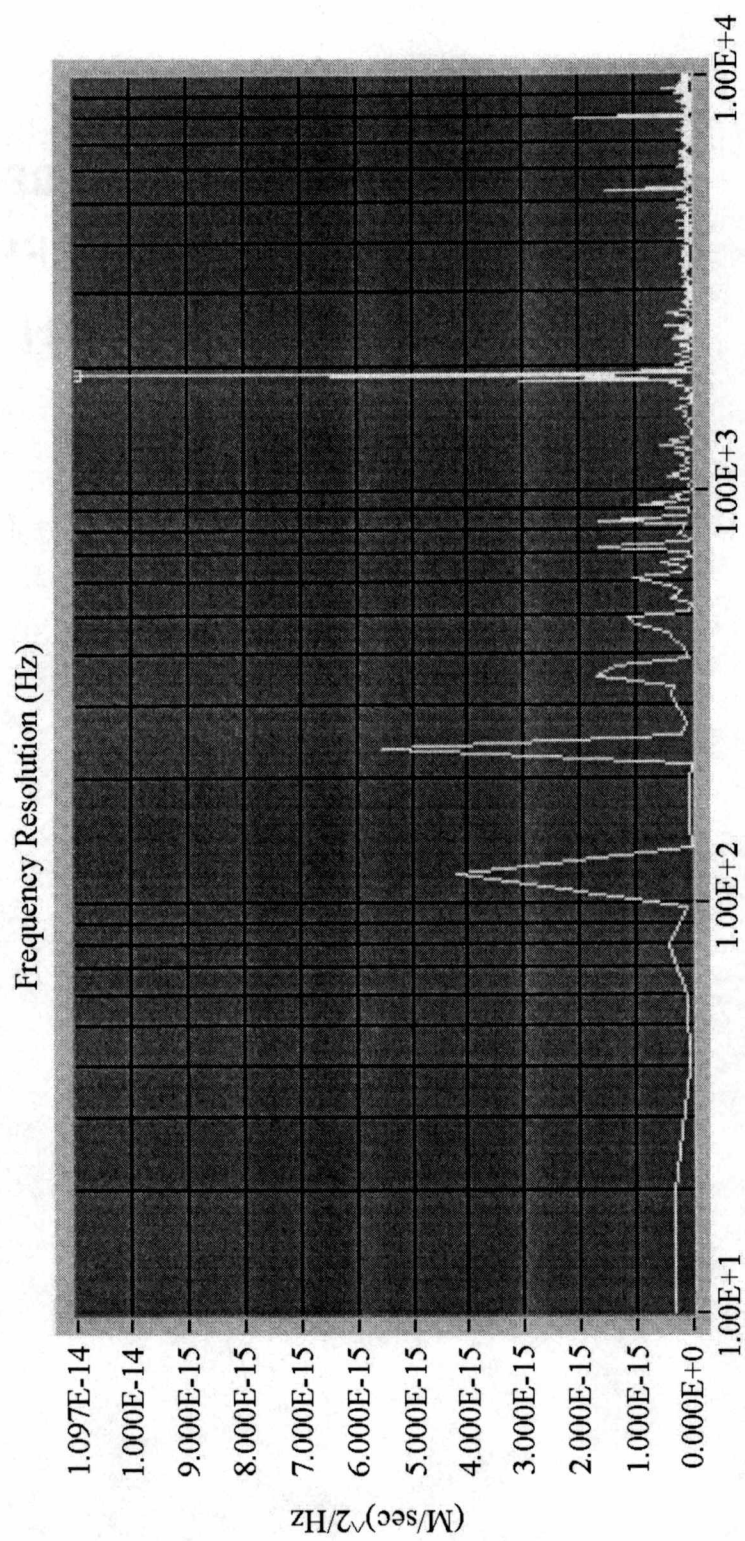
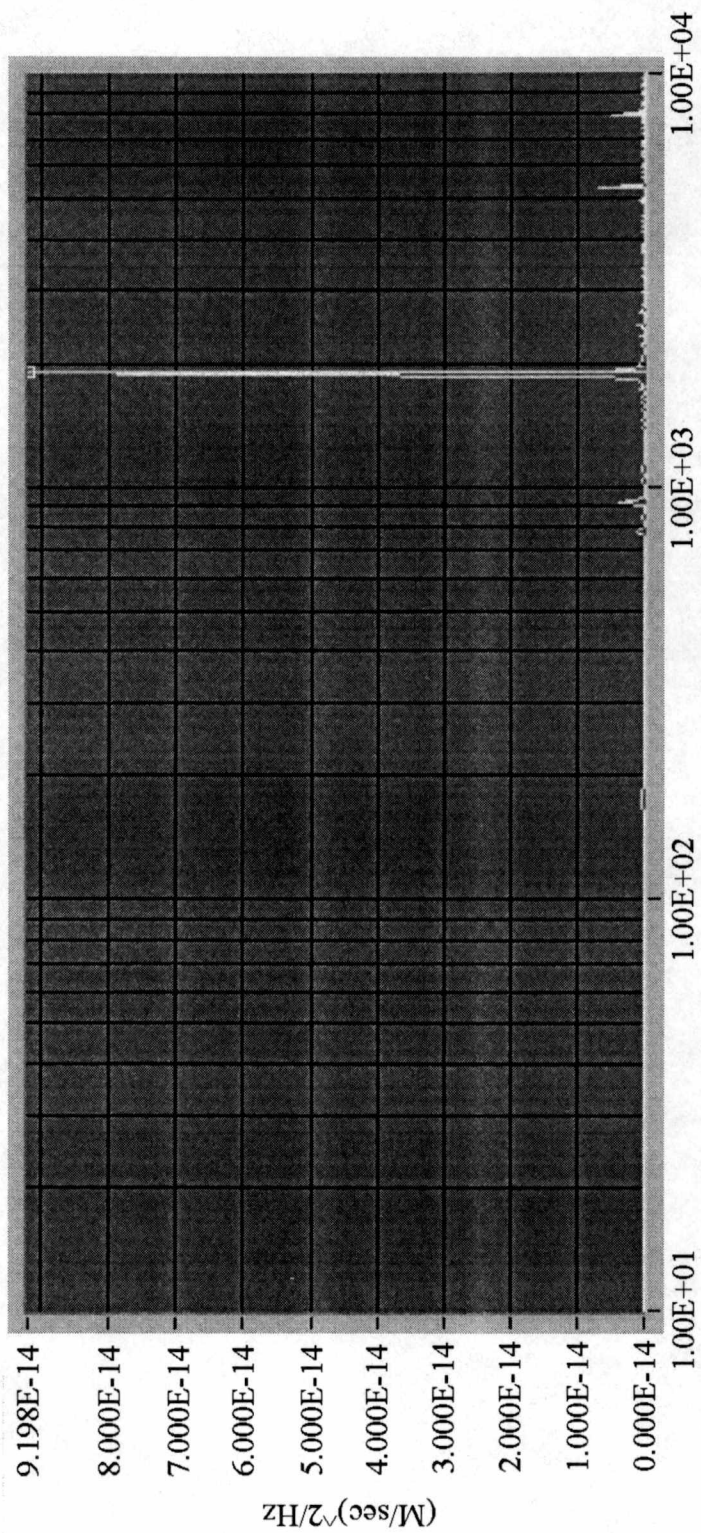


Figure 38: Fourier transform of the sound amplitude for the bat with a geometrical change centered at 31.54% from the barrel end of the bat. Most of the energy is contained in a single specific frequency.

Frequency Resolution (Hz)



6. CONCLUSION

This study has shown that internal geometrical changes to a bat will affect the frequency and vibration. The material and composition of the geometrical change affects the natural frequency of a bat. However, the utmost benefit of a geometrical change concerns its location in the bat.

For this study, it was determined from the bat's frequency analysis that a geometrical change centered at 31.54% from the barrel end of the bat was more beneficial than a geometrical change centered at either 40.36%, 49.19%, or 58.01% from the barrel end of the bat. The first two frequencies for the bat with a geometrical change centered at 31.54% were lower than any other frequencies for bats including the baseline model. The first two frequencies are the most important for this study because a change in these frequencies will in turn change the response of the bat after it has been impacted with a ball. This effect is very important when finding the optimum location for a geometrical change. Thus, based on results from this study, the location of the geometrical change centered at 31.54% from the barrel end is the optimum location.

By observing the time history analysis that was calculated for the baseline model bat and the two bats with a geometrical change centered at 31.54% and 40.36%, it is apparent there is a transient effect in the vibration behavior of the bat. As time increased, the amplitude of the displacement gradually began to reduce and the frequency started to decrease. This effect changed with the location of the geometrical change. The reduction in amplitude and the decrease in frequency was more pronounced for the geometrical

change centered at 31.54% than for the baseline model or for the geometrical change centered at 40.36% from the barrel end. Once again, it has been shown that an optimum location of the geometrical change will contribute significantly to the bat's behavior after an impact with a ball and for this study, a geometrical change centered at 31.54% is optimum.

The wall thickness of a bat also affects the frequency and vibration of the bat. For a bat with a wall thickness of 0.05 inchd as compared to a bat with a wall thickness of 0.1 inch, the first two frequencies are increased and the next two frequencies are decreased. The thinner walled bat also has amplitude of vibration greater than that of a thicker walled bat. The disadvantage to a very thin walled bat is that below a minimum wall thickness an impact will cause damage to the bat and the bat will vibrate more after impact.

The vibration of a bat is proportional to the sound amplitude produced from a ball and bat impact. Fourier transforms of the sound signals showed that for the baseline model, the frequency of vibration was distributed. For the bat with a geometrical change location of 31.54%, there was a single specific frequency of vibration. More energy will be present in the specific frequency in comparison to the energy that is distributed through the many frequencies of vibration. When energy is distributed through many frequencies, there is a loss of energy and this loss will be felt in the form of vibration. Thus, it has been shown that a geometrical change optimally located will improve the response of a bat after impact.

From all the analysis performed, it has been shown that geometrical changes in a bat are beneficial to reducing impact vibration. Not only is the addition of a geometrical change important, the location of the geometrical change is also crucial. With a geometrical change placed at an optimum location in a bat, the vibration in a bat will be reduced and, as a result, the size of the "sweet spot" will be increased.

BIBLIOGRAPHY

BIBLIOGRAPHY

- Ali, H. E. M. and I. M. Traina. COSMOS/M Basic System Guide Volume 3. Santa Monica, California: Structural Research and Analysis Corporation, 1996.
- Ali, H. E. M. and I. M. Traina. COSMOS/M Theoretical Manual. Santa Monica, California: Structural Research and Analysis Corporation, 1996.
- Ali, H. E. M. and I. M. Traina. COSMOS/M Finite Element Analysis System: User Guide. First Edition. Santa Monica, California: Structural Research and Analysis Corporation, 1993.
- Ali, H. E. M. and I. M. Traina. COSMOS/M Advanced Modules. Santa Monica, California: Structural Research and Analysis Corporation, 1996.
- Adair, Robert K. Physics of Baseball. New York, New York: Harper and Row Publishers, Inc., 1990.
- Ashley, Steven. "Taking a Swing with Three-Piece Bats." Mechanical Engineering (1995): 86-87.
- Beer, Ferdinand P. and E. Russel Johnston, Jr. Mechanics of Materials. Second Edition. New York, New York: McGraw Hill, Inc., 1992.
- Berry, Michael J., Stephen P. Messier, Brian S. Ruhmann, and Andrew S. Weyrich. "Effects of Bat Composition, Grip Firmness, and Impact Location on Postimpact Ball Velocity." Medicine and Science in Sports and Medicine 21 (1988): 199-205.
- Brody, Howard. "Models of Baseball Bats." American Journal of Physics 58 (1990): 756-758.
- Brody, Howard. "The Sweet Spot of a Baseball Bat." American Journal of Physics 54 (1986): 640-643.
- Burden, Richard L. and J. Douglas Faires. Numerical Analysis. Fifth Edition. Boston, Massachusetts: PWS Publishing Company, 1993.
- Dunbar, Eric and David Tognarelli. "How Sweet It Is!! – Can Your Baseball Bat Measure Up?" Sound and Vibration (1994): 6-16.
- Hester, Leslie R. and Keith Koenig. "Performance Measurement of Baseball Bats." Journal of the Mississippi Academy 38 (1993): 7-10.
- Ingard, K. Uno and Philip M Morse. Theoretical Acoustics. New York, New York: McGraw Hill, Inc., 1968.

- Kirkpatrick, Paul. "Batting the Ball." American Journal of Physics 31 (1963): 606-613.
- Noble, L. "Empirical Determination of the Center of Percussion Axis of Softball and Baseball Bats." International Series on Biomechanics 5 (1985): 516-520.
- Noble, Larry and Hugh Walker. "Baseball Bat Inertial and Vibrational Characteristics and Discomfort Following Ball-Bat Impacts." Journal of Applied Biomechanics 10 (1994): 132-144.
- Riley, William F. and Leroy D. Sturges. Dynamics. New York, New York: John Wiley and Sons, Inc., 1993.
- Schuessler, Raymond. "'Only the Finest New York Ash' A Brief History of the Baseball Bat." The Northern Logger and Timber Processor (1994): 32-33.
- Van Zandt, L. L. "The Dynamical Theory of the Baseball Bat." American Journal of Physics 60 (1992): 172-181.

VITA

Holley Lagay Britton was born in Huntsville, Alabama on June 27, 1972. She is the only child of Charlie and Vera Britton. Holley grew up on a cattle farm in Hazel Green, Alabama.

She attended private schools in Huntsville, Alabama including the college preparatory school, Randolph. In May of 1990, she graduated with honors from Randolph. Holley was involved in many activities at Randolph. She was the senior class secretary, a member of the National Honor Society, the secretary of Mu Alpha Theta, a member of the Spanish National Honor Society, a captain of varsity girls basketball team her senior year, a member of the Fellowship of Christian Athletes, and a member of the tennis team.

Holley received a National Merit Scholarship to be used at the college of her choice. She also accepted a scholarship from the University of Alabama in Huntsville, which she chose as the college of her choice. She began her studies with the hope of someday becoming a physical therapist. However, after two years she changed her major to mechanical engineering. In May of 1996, Holley graduated with a Bachelor of Science in Mechanical Engineering from the University of Alabama in Huntsville.

While attending the university, she was involved in many design projects. Holley was on a four-member team that designed and built a fully suspended mountain bike. She was also on a team of three that designed and built the frame for a mini baja. An upper stage hybrid rocket motor was also a design project in which she participated. For this project, Holley was in charge of the configuration layout.

Throughout Holley's undergraduate years, she had several different jobs. She was an assistant varsity girl's basketball coach at Randolph for two years. She then was hired as the head 7th grade girl's basketball team. Holley was also a sales associate at a clothing store, the GAP. While employed by the GAP, she received several awards including a pin of merit for having the single highest sale. Holley also worked for Dr. Clark Hawk, head of rocket propulsion at the University of Alabama in Huntsville. She did research on Fresnel lenses and worked in the university's optics lab.

After graduating from college, Holley entered The University of Tennessee Space Institute in Tullahoma, Tennessee to pursue a Master of Science in Mechanical Engineering. The master degree was received in December 1998.